published estimates, much closer to the water budget estimates than found using the specified recharge domain approach attempted in the first model (Section 4.2.5).

Recharge was applied to the active parts of Layer 3 outside the active portion of Layer 1 in both models. This boundary condition was intended to model percolation to the water table and vertical leakage through all of the overlying units to the Mahomet Aquifer beyond the area in which the Glasford Formation was explicitly modeled.

River boundaries In the first model, all of the rivers shown in Figure 24 were explicitly modeled. These are the rivers that are known or inferred to discharge to or receive discharge from the Mahomet Aquifer. In the second model, each cell in Layer 1 has a river boundary condition that is intended to capture the effects of both areal recharge to the aquifer and discharge to and from rivers. Consequently, the Sangamon River and the Vermilion River were explicitly modeled as the lowest reaches in the water table aquifer. The effect of this approach to modeling recharge is that the upper aquifer will be a sink at the streams and rivers (where heads were lowest) and it will allow more water into the Glasford as heads in the Glasford decline.

Only the rivers beyond the limits of the active area of Layer 1 were explicitly modeled as connected to Layer 3 in both models.

Wells The wells shown in Figure 25 are from the ISWS public water supply database. These wells were included in the groundwater flow model. Those wells outside the limits of the Mahomet Aquifer were not included in the model. Locations of other categories of withdrawal described in the Demand Analysis (industrial, commercial, agricultural, etc.) were not available so these withdrawal were not modeled explicitly. The vast majority of agricultural withdrawal occurs in the western Mahomet Aquifer region; and much of this withdrawal is near the Illinois River and the lower Sangamon River in Mason and Tazewell Counties (Figure 12). For the purposes of our modeling, the recharge and river boundary conditions in the western Mahomet Aquifer adequately capture the effects of agricultural pumping in this area. In order to account for the uncertainty in total withdrawal from the aquifer in other areas, a scale factor was applied to the rate of each known well (Section 4.2.1).

4.1.4 Other model control variables

Layer 1 of the MODFLOW model was defined as a convertible model layer – confined if the computed head is above the top of the layer and unconfined otherwise. Layers 2 and 3 were defined as confined model layers.

Cell drying was not allowed for Layer 1. When the head in a model cell falls below the bottom of the layer, the head is fixed at the elevation of the base of the cell. In this way, the transmissivity

of the model layer becomes 0 and the instability caused by cells re–wetting and drying in successive iterations is avoided.

The head convergence criteria used was typically $1 \times 10^{-5}\ ft$; such a low value is required when using PEST as described in the following section. For simulations of the new wellfield, the model was set to converge even if this low tolerance was not met. Even in cases where the tight convergence tolerance was not met, the percent discrepancy on the overall flow budget for steady–state models was less than 0.1 percent.

For transient simulations, the head convergence criteria used was set to $1 \times 10^{-6}\ ft$ and the flow residual convergence tolerance was placed as low as $1 \times 10^{-8}\ ft^3/day$. Biased time–stepping was used and the initial time step was set lower than the critical value described by Anderson and Woessner [1992, p. 205]. For the simulation of the Visocky pumping test, the percent discrepancy on the overall model budget exceeded 1 percent for the first few time steps, but later in the simulation these discrepancies dropped well below 0.1 percent.

4.2 Model calibration

The software package PEST [Doherty, 2004] was used in model calibration. PEST uses a modified Gauss–Marquardt–Levenberg method of non–linear least squares to determine a parameter set that minimizes the sum of squared, weighted residuals. Residuals are the difference between observed and simulated values for the data described above. These differences are summarized as the objective function (Φ) which is a scalar value that PEST seeks to minimize during a typical parameter estimation run; Φ is defined in Equation 2.

$$\Phi = \sum_{i=1}^{m} [(o_i - c_i) w_i]^2 \tag{2}$$

where:

m is the number of observations used in the calibration

o_i is an observation consisting of a measured or estimated value the model is being used to simulate

c_i is the corresponding modeled value

$o_i - c_i$ is the residual associated with observation i

w_i is the weight associated with observation i.

This process did not operate on auto pilot. Calibration of the groundwater flow model was done using a combination of manual and automated methods. A series of water level observations were identified from the ISWS data along with published aquifer test data that were matched by optimizing parameter values used in the model. Details are presented in the following subsections.

Anthropogenic changes on the system are so pervasive that calibration of the system is highly dependent on the accuracy of the groundwater withdrawal information. Withdrawal for irrigation is unreported. Industrial withdrawal information is generalized to the township. Water level data from pumping wells that are temporarily idle are suspect because the water level may not have fully recovered to a representative value. Water level data from widely distributed wells are not likely to have been collected at the same time.

Water levels in the Mahomet Aquifer have declined over time due to increased rates of withdrawal and reduction of storage of water in the aquifer system. Sufficient data to differentiate between these causes is not currently available. Despite these shortcomings, the calibrated model was the best tool available for our evaluation of the new wellfield.

4.2.1 Parameters

Parameters varied during the model calibration are described in this section. The calibrated values for the second conceptual model described in Section 4.1.3 are listed in Table 20. These values are consistent with regional information summarized in Section 3.2 and Tables 18 and 19.

Hydraulic conductivity Zones of uniform hydraulic conductivity were defined within the model layer representing the Glasford Aquifer as follows:

1. a zone representing areas in which neither sand unit was mapped – this is inferred to be a low–conductivity zone that tends to limit the lateral flow of water in the Glasford Aquifer (see Figure 17);
2. a zone representing areas in which only the Vandalia Sand was mapped;
3. a zone representing areas in which only the Radnor Sand was mapped;
4. a zone representing areas in which both the Vandalia Sand and the Radnor Sand were mapped. This zone was set equal to the zone representing the Vandalia Sand in order to reduce the number of model parameters varied during the calibration.

Representative hydraulic conductivity values for the zones in the Glasford Aquifer was estimated using the Equation 3 which is from Anderson and Woessner (1992, p. 69). This assumes each zone is a two–layered system – one layer being the sand layer mapped by Soller et al. [1999] and the other layer being lower hydraulic conductivity material (glacial till).

$$K_{eff} = \frac{K_{sand} \cdot b_{sand} + K_{till} \cdot b_{till}}{b_{sand} + b_{till}} \tag{3}$$

where:

K_{eff} is the effective horizontal hydraulic conductivity of the layered system

K_{sand} is the horizontal hydraulic conductivity of the sand layer

K_{till} is the horizontal hydraulic conductivity of the till layer

b_{sand} is the saturated thickness of the sand layer

b_{till} is the saturated thickness of the till layer

Layers 2 and 3 have uniform hydraulic conductivity with the exception of a zone of lower hydraulic conductivity in Layer 3 north of Champaign/Urbana (Figure 23). This zone was established based on information presented by the ISWS.

Storage parameters MODFLOW-2000 uses specific storage rather than storage coefficient for confined and convertible aquifer layers [Harbaugh et al., 2000]. Specific storage was calculated by dividing the storage coefficient value of 3.1×10^{-4} from the aquifer test of the Petro Well reported by Visocky and Schicht [1969] by the layer thicknesses. Layer 1 was assigned a specific yield value of 0.1. The storage parameters were not adjusted during the model calibration.

Riverbed conductance for linear features Riverbed conductance and resistance are related parameters that both describe flow between a river and a underlying aquifer. For linear features, GMS expresses this parameter in terms of conductance per unit length for linear features ($ft^2/day \cdot ft$). Conductance of a river bed deposit (C) is defined as $C \equiv KA/L$, where K is the vertical hydraulic conductivity, A is the area under consideration, and L is the vertical thickness of the deposit. GMS calculates the length of an arc representing a river within a given model cell. This length is multiplied by a parameter representing the width of the river and the thickness of the vertical hydraulic conductivity of the riverbed deposits. In our model, the conductance multiplier is also intended to represent the effects of the material between the river of interest and the aquifer layer to which the river is assumed to be connected.

Five riverbed conductance parameters were defined for the first conceptual model. The distribution is described in the following list and shown on Figure 24. The second conceptual model included only those rivers assumed to be connected to Layer 3.

- A conductance multiplier for the Sangamon River upstream of the town of Mahomet – applied to model Layer 1.
- A conductance multiplier for the Sangamon River downstream of the town of Mahomet – applied to model Layer 1.
- A conductance multiplier for the Vermilion River – applied to model Layer 1.

- A conductance multiplier for the Iroquois River and tributary – applied to model Layer 3.
- A conductance multiplier for the Illinois River – applied to model Layer 3.

Riverbed conductance for entire model cells As described in Section 4.1.3, the second conceptual model used the MODFLOW river package to model recharge in each active cell in Layer 1. In this case, the riverbed conductance parameter for Layer 1 represented the effective hydraulic conductivity for the material above the Glasford Aquifer divided by the thickness of this material ($ft/day \cdot ft$). This parameter was applied uniformly over the model layer by multiplying by the cell area to produce the conductance value used by MODFLOW.

Recharge In the first conceptual model, recharge zones were defined on both Layers 1 and 3 of the model. In the area in which Layer 1 is active, three zones were defined: one that is underlain by the Vandalia Sand, one that is underlain by the Radnor Sand, and one that is underlain by neither sand. In the second conceptual model, the recharge package was not used to introduce water into Layer 1. In both conceptual models, recharge is applied directly to Layer 3 in the active areas of Layer 3 beyond the limits of the active area of Layer 1.

Pumping rates Due to the uncertainty regarding the pumping database (see the Demand Analysis report for additional information), a scaling factor was applied to the known public water supply pumping from the Mahomet Aquifer. In this way, the effects of unaccounted withdrawal and the possible bias between the average annual rates and the water level measurements (which may occur during periods of high withdrawal) could be addressed. The scale factor was allowed to range between 1 and 2.5. The scale factor caused the modeled discharge values for the ILAW wellfields to be closer to the maximum daily rates than the annual average rates described in Section 2.1.

4.2.2 Observations

Water level data supplied by the ISWS were used as observations in the model calibration (see Figure 18), along with information from an aquifer test data from a test west of Champaign [see Figure 13 of Visocky and Schicht, 1969]. This test was located approximately 1.5 miles east of Bondville and showed a strong leaky–confined signature. The aquifer parameters determined from this test were used to calculate a time–drawdown data set for an observation well located exactly 6 model cells from the pumping well (1980 ft). In this way, the accuracy of the MODFLOW solution is not compromised by interpolating between adjacent cells. A plot of modeled and observed time–drawdown is shown in Figure 26.

It should be noted that although the drawdown at the end of the 24–hour test was approximately 2.5 ft, the steady–state solution has a drawdown of 10.4 ft at the position of the observation well.

This is a reflection of the 3–dimensional complexity of the problem and is consistent with ISWS observations of an aquifer test near the town of Monticello [Roadcap and Wilson, 2004]. Dewatering of shallow water–bearing zones will affect some local wells and will ultimately reduce the capacity of the Mahomet Aquifer due to decreased vertical leakage.

Contour maps of measured and modeled water levels in the Mahomet Aquifer are shown in Figures 27A and B, respectively. A scatter plot of measured and observed water levels from the steady–state model calibration is shown in Figure 28.

4.2.3 Prior information

Prior information in model calibration consists of independent estimates of model parameter values. Articles of prior information were included regarding the effective hydraulic conductivity of the zones in Layer 1 representing the Radnor and Vandalia Sands and the hydraulic conductivity of the Mahomet Aquifer. The hydraulic conductivity values for the Radnor and Vandalia Sands were calculated using Equation 3 with a value of 220 ft/day for the hydraulic conductivity of the sand layers, 10 ft/day for the hydraulic conductivity of the till, a typical saturated thickness of 20 ft for the sand layers, and a typical saturated thickness of 100 ft for the till. The value for the Mahomet Aquifer hydraulic conductivity was determined by dividing the transmissivity reported by Visocky and Schicht [1969, Figure 13] by a model layer thickness in that cell of 130 ft.

4.2.4 Independent model prediction

We included an independent model prediction in the model calibration run. This prediction was the average drawdown in the Mahomet Aquifer beneath all known Glasford Aquifer wells caused by new wells west of the West Wellfield pumping at a combined rate of 20 MGD. This approach is the basis for predictive analysis as described in Section 4.3. This prediction was treated as an observation during the model calibration and a value provided to PEST that would push the calibration toward maximizing this drawdown in order to make the analysis conservative. This method is called dual calibration by Doherty [2004, Section 6.1.5].

4.2.5 Budget summary

A summary of the water budgets for the calibrated model representing 2004 conditions and a simulation representing the proposed wellfield pumping is presented in Table 21. The model of the new wellfield includes eight wells pumping at a combined rate of 20 MGD with the existing wells in the West Wellfield scaled back a total of 4 MGD.

The net inflow to Layer 1 of the calibrated model is roughly $1/4$ of regional estimates for the Glasford Aquifer (see Section 3.2.1) but the model does not incorporate mechanisms such as localized zone of higher infiltration described by Roadcap and Wilson [2004] that would tend to

increase the amount of recharge to the Glasford. In addition, no withdrawal from the Glasford is modeled. Such withdrawal would have to be offset by additional recharge to the aquifer.

Layer 2 contains no sources or sinks. Excess water from Layer 1 passes through Layer 2 to Layer 3. In a few model cells, water passed from Layer 3, through Layer 2 and discharged to river cells connected to Layer 1. The net flow direction was downward through Layer 2.

Like Layer 1, the net inflow to Layer 3 of the model is lower than regional estimates with 0.17 to 0.38 in/yr reaching the Mahomet Aquifer compared to an estimated value of 2.2 in/yr (see Section 3.2.1). Unaccounted withdrawal from the Mahomet Aquifer would have to be offset by additional recharge to the aquifer. Groundwater discharge to the Illinois River and Iroquois River divided by the modeled area of the aquifer is 0.16 in/yr.

4.3 Predictive analysis

The method of predictive analysis described by Doherty [2004, Section 6] was applied manually to estimate a worst–case well interference for the new wellfield based on a preliminary layout. Predictive analysis follows model calibration and uses information from the calibration to determine a likely range of values for an independent prediction. In this case, the independent prediction was the average steady–state drawdown in the Mahomet Aquifer beneath wells completed in the Glasford Aquifer due to pumping a new wellfield west of Champaign at 20 MGD. As described in Section 5, these are the wells that are most vulnerable to being rendered unusable. This independent prediction is maximized while keeping the model essentially calibrated.

In predictive analysis, the user specifies an increment to the objective function δ, which is a statistically–derived number based on Equation 4[Doherty, 2004].

$$\delta = \frac{\Phi_{min}}{m-n} F_{\alpha}(n, m-n) \tag{4}$$

where:

Φ_{min} is the minimum value of the objective function obtained during the model calibration

m is the number of observations used in the calibration

n is the number of parameters being calibrated

$F()$ is the critical value for the $F-test$

α is the level of certainty specified for the analysis.

The purpose of the increment δ is to define a value for the objective function $\Phi_{min} + \delta$ that represents a specific uncertainty associated with the model calibration. For the first conceptual model, the average drawdown in the Mahomet Aquifer is most sensitive to the conductance parameter for the reach

of the Sangamon River below the town of Mahomet. This is consistent with information from the ISWS regarding vertical leakage to the Mahomet Aquifer in this area [Roadcap and Wilson, 2004]. For the second conceptual model, the average drawdown in the Mahomet Aquifer is most sensitive to the conductance multiplier for the river cells on Layer 1. This parameter was lowered until the objective function rose to approximately $\Phi_{min} + \delta$. The influence of this change on the model prediction is described in Section 5.2.1.

4.4 Discussion

Our experience in calibrating the flow model based on the first conceptual model was that we could not put as much recharge on the Glasford Aquifer as regional information would suggest we should. This is due in large part to the lack of a mechanism for simulated localized discharge in subdrainages or agricultural drains as described in Section 4.1.3. In addition, the hydraulic conductivity of the zones in Layer 1 tended to converge on high values in order to lower heads in this layer. This is why the second conceptual model was adopted.

Any future modeling should include a hybrid between these approaches in which zones of river cell conductance and or hydraulic conductivity in Layer 2 are established that reflect the variability of the hydraulic connection between the rivers and the Glasford and Mahomet Aquifers.

Modeled gradients in the Mahomet Aquifer were much steeper than observed in the narrow "throat" to the West of Champaign County. In general, far–field aquifer properties are less important than in the near–field but in this case the high transmissivity in this part of the aquifer could alter local findings. Conditions that exist may limit regional drawdown from the proposed wellfield to the West. This high–transmissivity area should be explicitly evaluated in future regional groundwater modeling to better understand regional flow through this narrow reach of the buried valley aquifer.

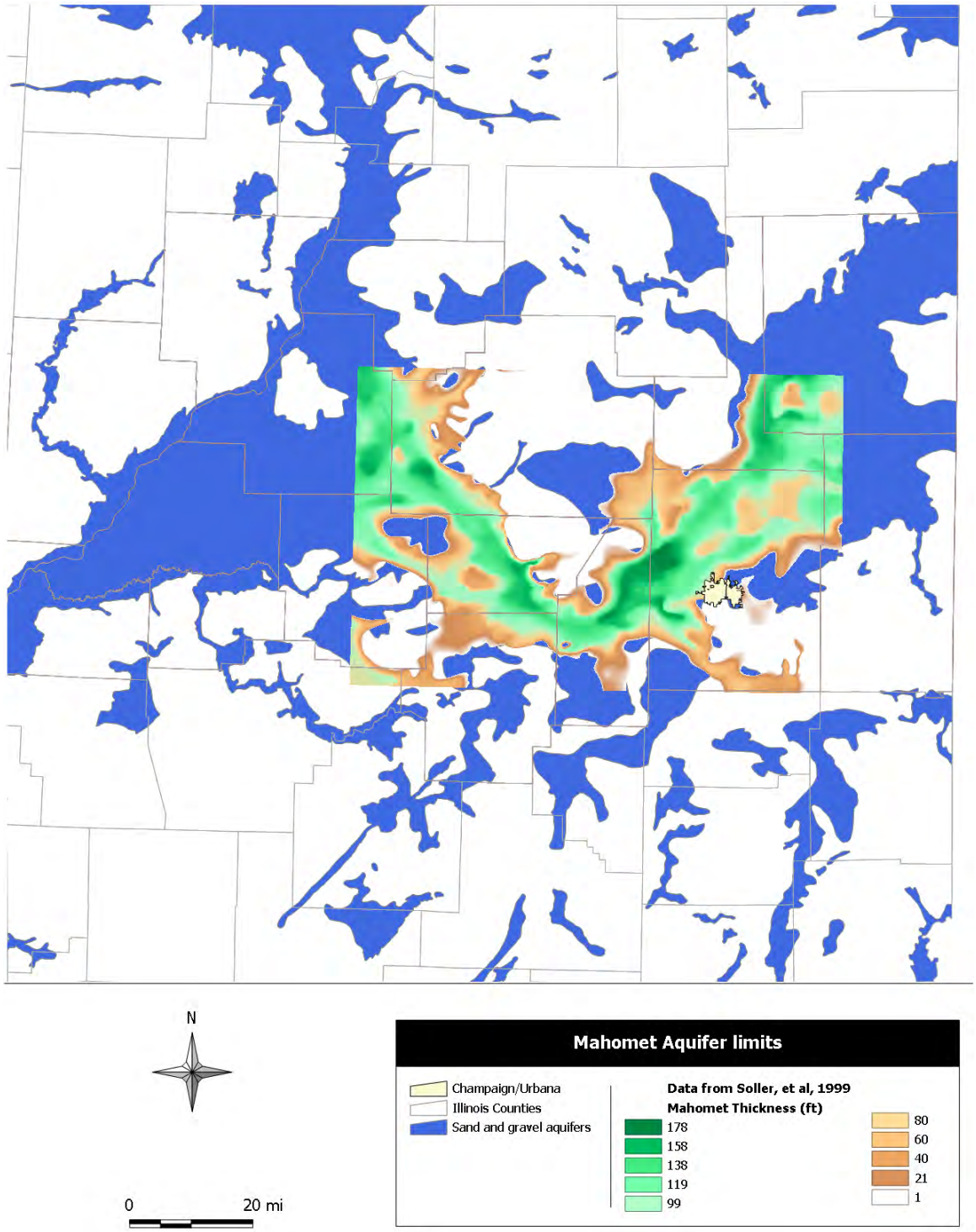

Figure 20: Location of project, limits of data from [Soller et al., 1999], and extent of Quaternary aquifers east-central Illinois.

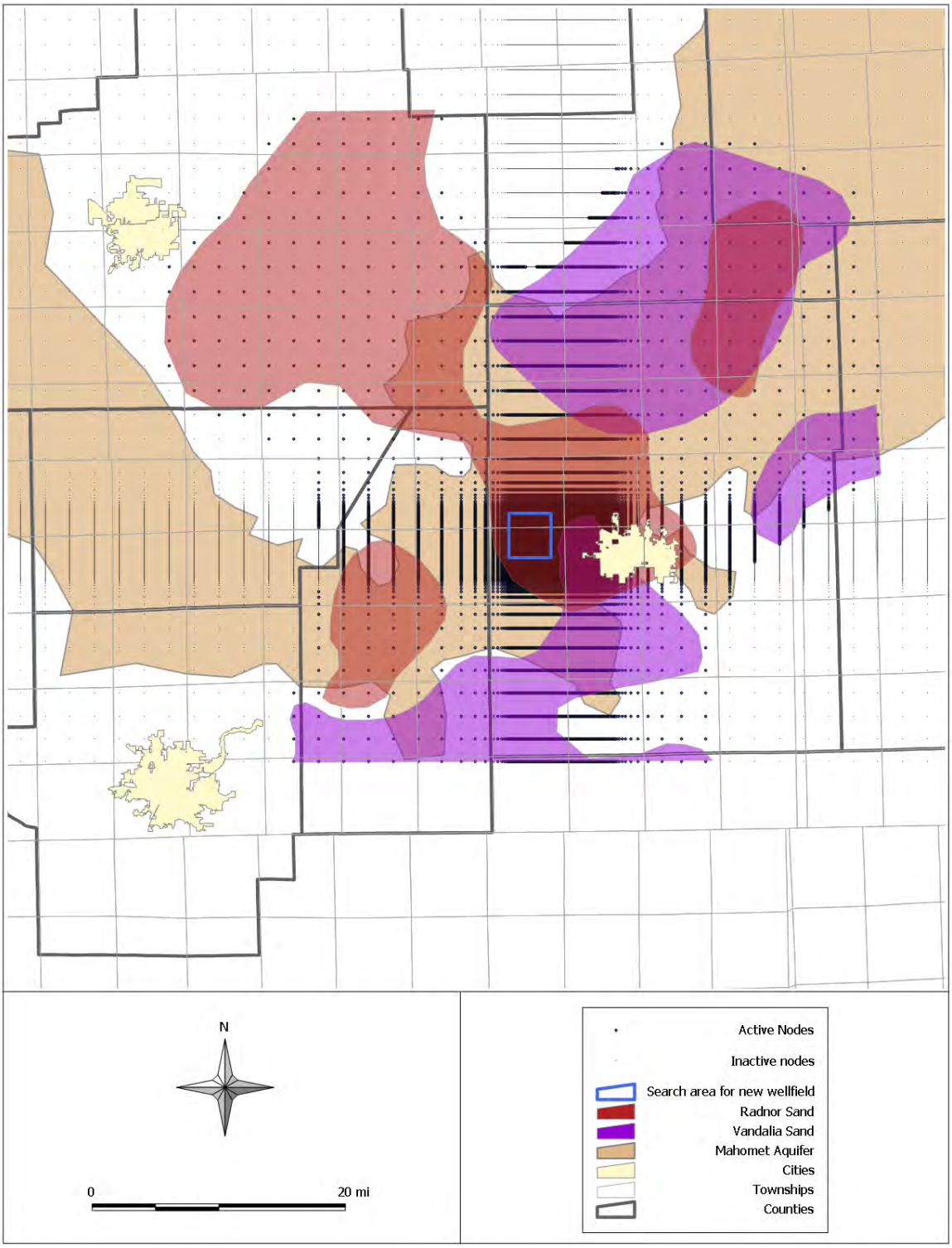

Figure 21: Model grid for Layer 1 with hydraulic conductivity zones in Layers 1 and 3.

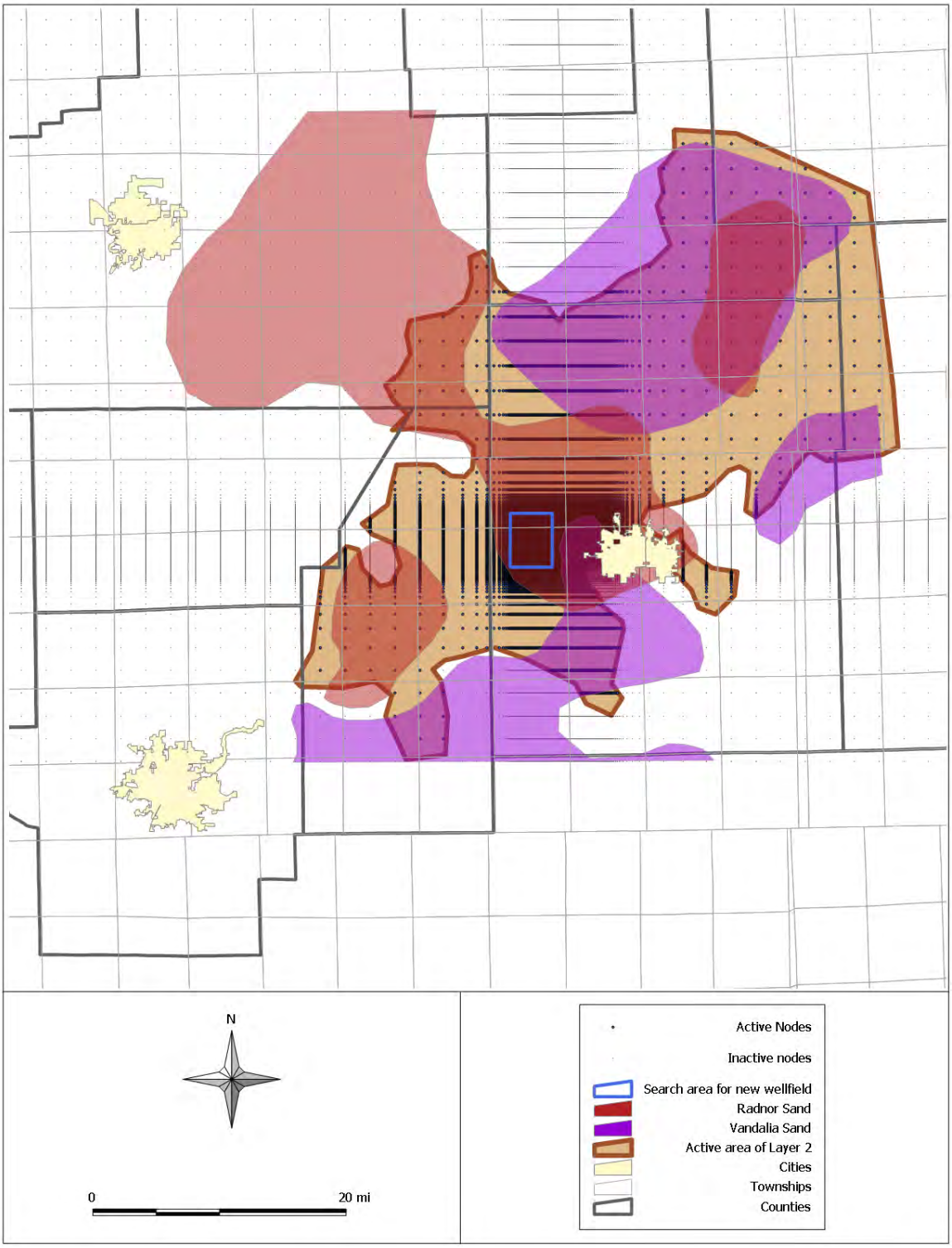

Figure 22: Model grid for Layer 2 with hydraulic conductivity zones in Layers 1 and 3.

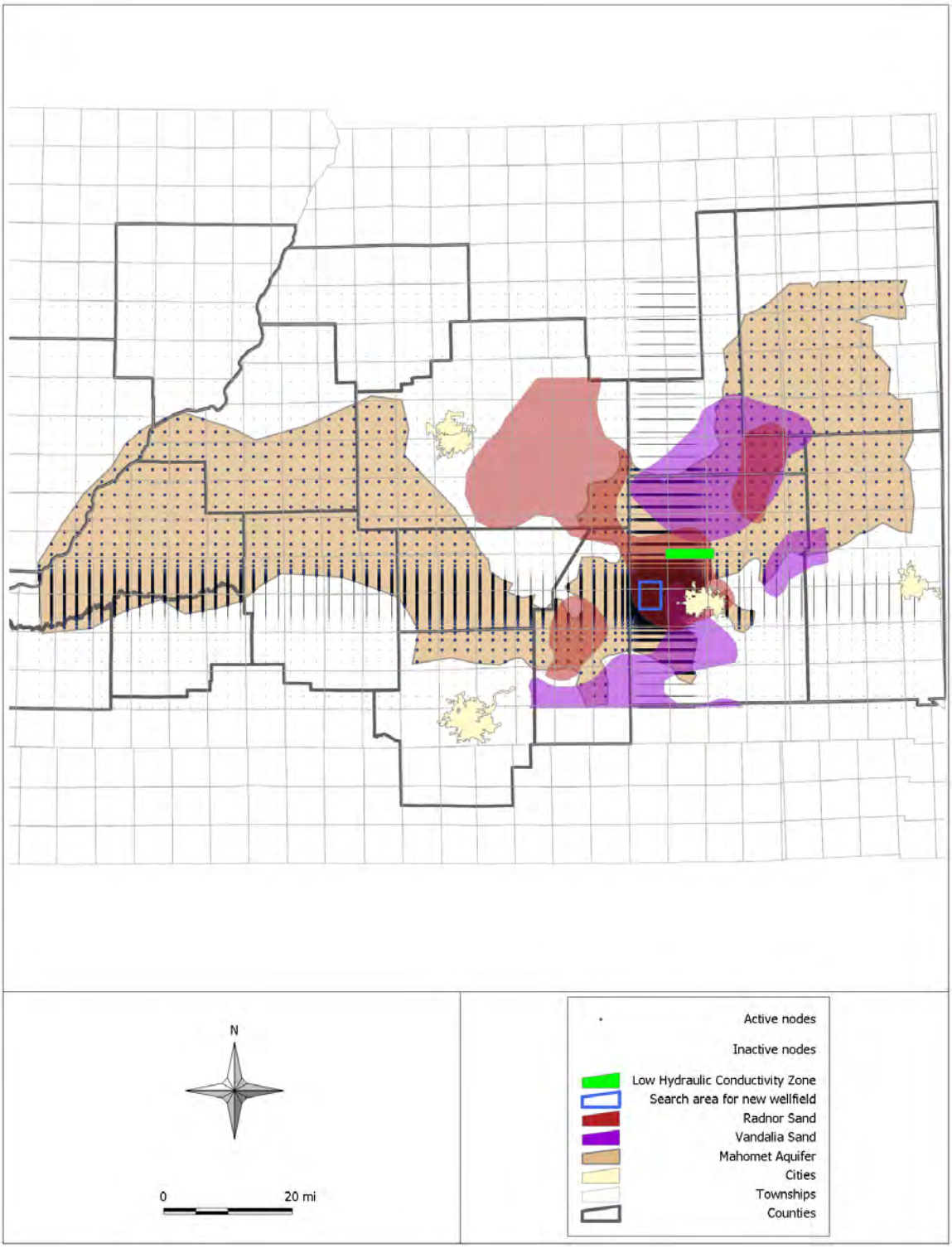

Figure 23: Model grid for Layer 3 with hydraulic conductivity zones in Layers 1 and 3.

Table 18: Aquifer parameter estimates from Visocky and Schicht, 1969

Location	Saturated thickness (ft)	Transmissivity (ft^2/day)	Horizontal hydraulic conductivity (ft/day)	Storage coefficient ($unitless$)	Confining bed thickness (ft)	Vertical hydraulic conductivity (ft/day)	Characteristic leakage length (λ) (ft)
Glasford Aquifer							
Selected aquifer test results from Champaign County							
Tolono	40	1890	47	1.7E-4			
Swift&Co.	38	8480	223	1.0E-5			
St. Joseph	16	1740	109	1.0E-4	34	4.7E-3	
State of Ill.	8	450	56	2.2E-4			
Clifford Jacobs Forging	21	3060	146	3.5E-3	24	4.2E+0	
Results of wellfield case history analyses							
Arcola	20	1340	67	NA	70	5.3E-3	
Hoopeston	52	19000	370	NA	60	5.2E-3	
Rantoul	50	9600	190	NA	80	3.5E-4	
Mahomet Aquifer							
Selected aquifer test results from Champaign County							
No. Ill. Water Corp.	100	43450	435	4.1E-4	35	2.4E-2	8,000
Petro Chemicals Corp.	75	33690	449	3.1E-4	35	2.9E-2	6,400
Petro Chemicals Corp.	83	31550	380	3.1E-4	50	5.6E-2	5,300
No. Ill. Water Corp.	90	43450	483	4.1E-4	35	2.4E-2	8,000
Results of wellfield case history analyses							
Fisher	90	10200	110	NA	87	5.3E-3	12,900
Monticello	94	26700	280	NA	60	3.1E-3	22,800
Rantoul	55	18000	330	NA	75	6.7E-4	44,900
Watseka	45	27000	600	NA	100	1.3E-3	44,900

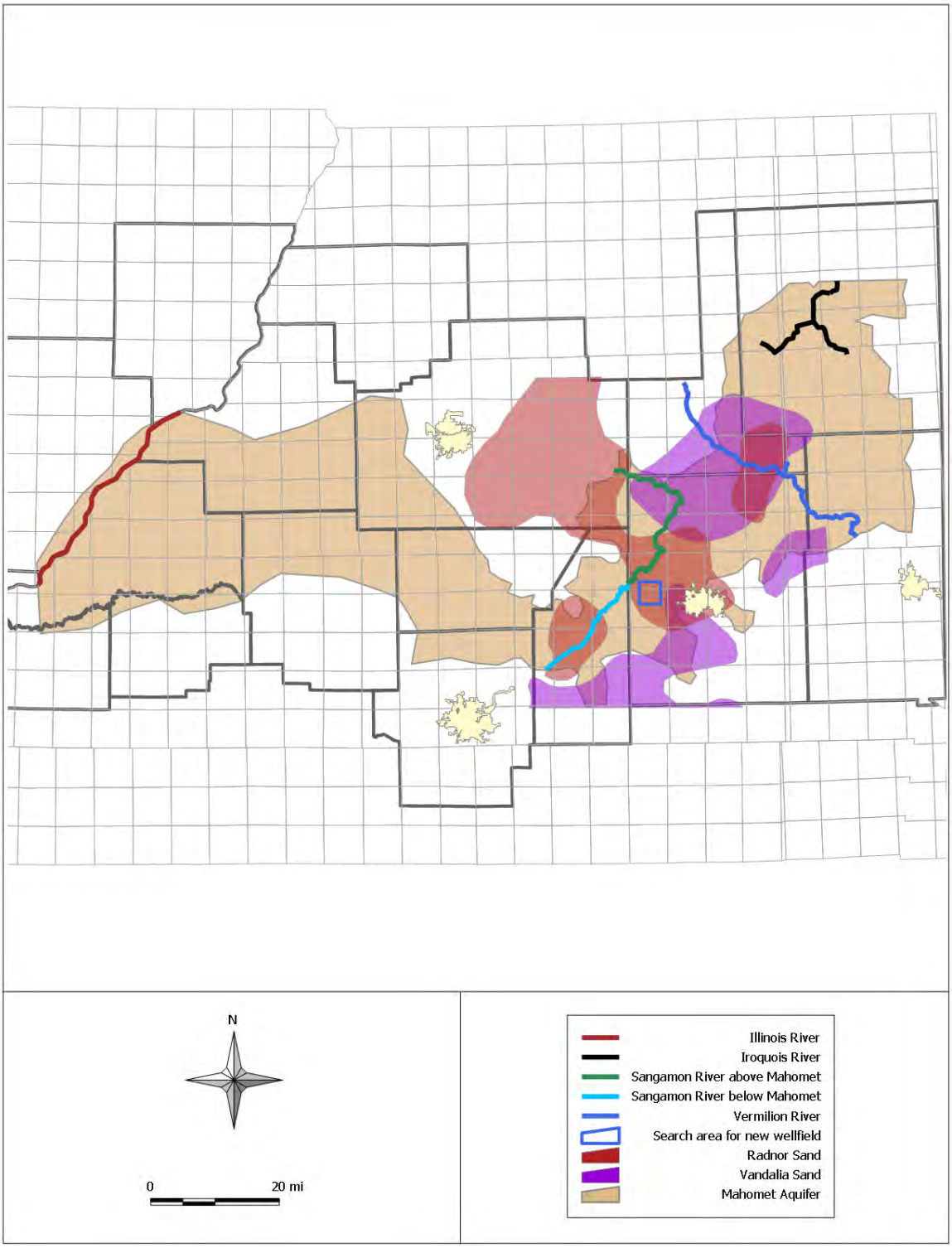

Figure 24: Location of rivers included in the groundwater flow model.

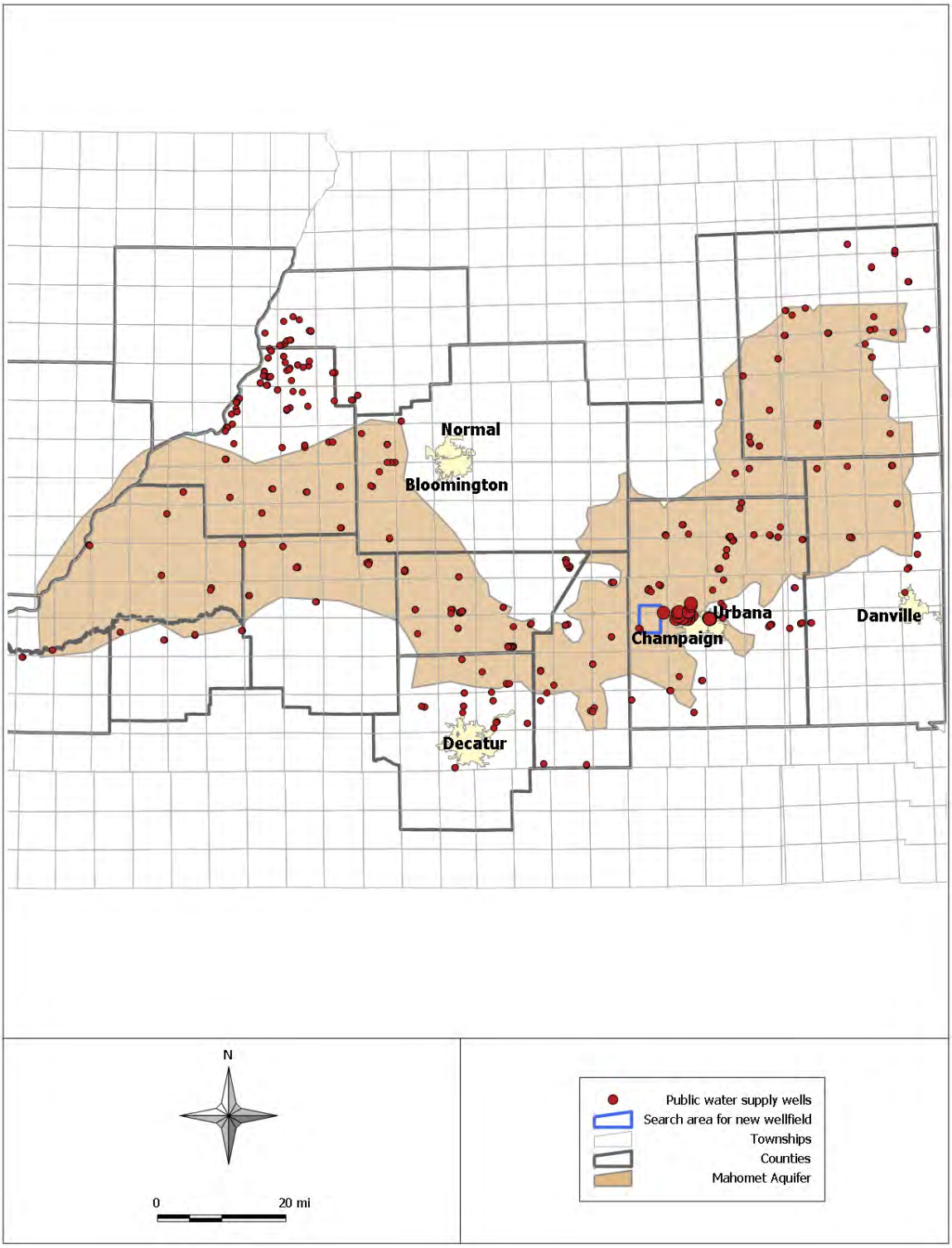

Figure 25: Public water supply wells included in the groundwater flow model.

Table 19: Aquifer parameter estimates from Kempton et al., 1991

Description	Transmissivity (ft^2/day)	Horizontal hydraulic conductivity (ft/day)	Storage coefficient ($unitless$)	Vertical hydraulic conductivity (ft/day)
Glasford Aquifer/confining layers				
minimum			1.5E-5	2.8E-4
maximum	31,100	620	8.0E-2	5.3E-2
Mahomet Aquifer				
minimum			2.0E-5	
maximum	68,200	570	2.0E-3	

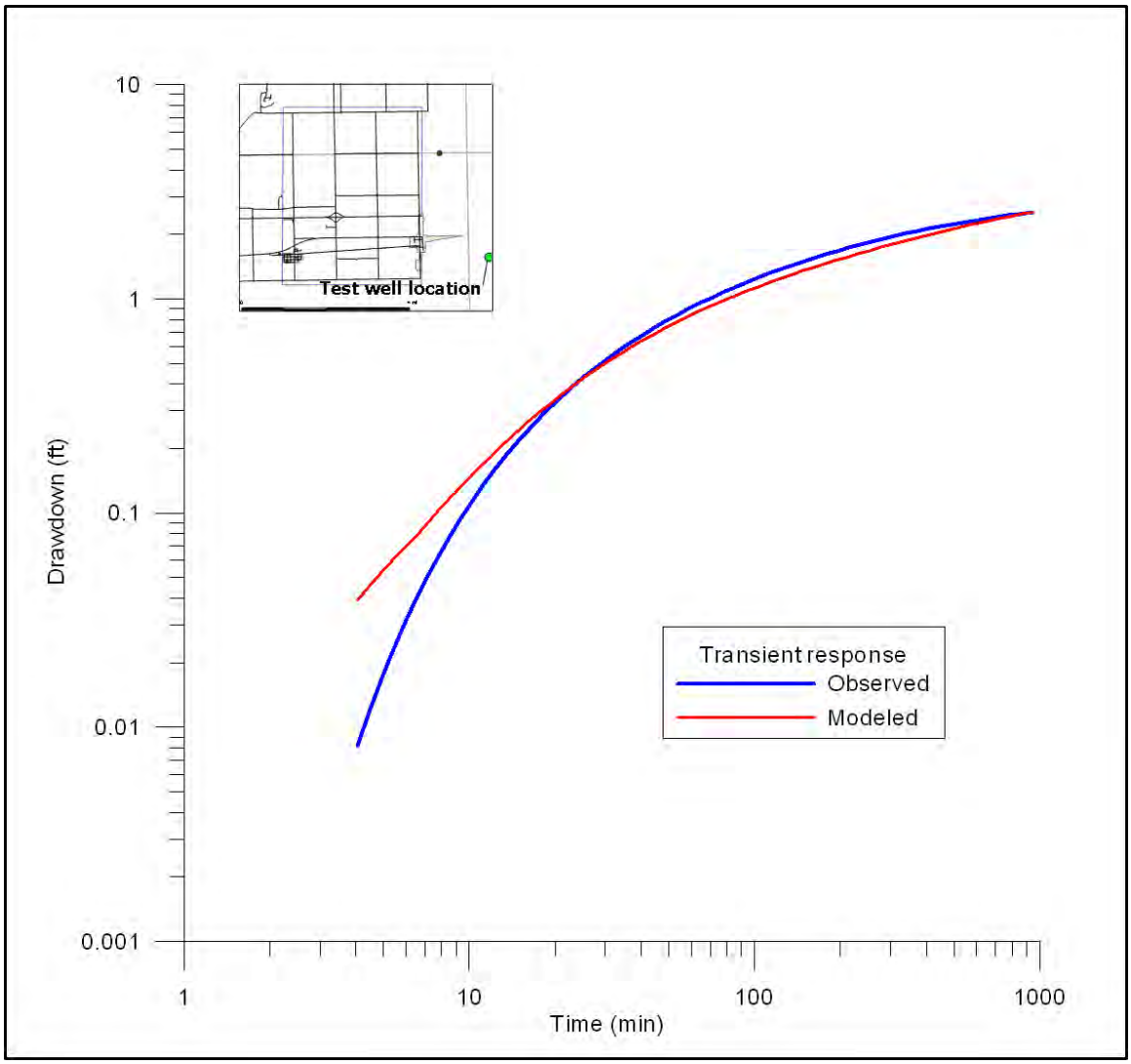

Figure 26: Plot of measured and observed drawdown in response to an aquifer test in the Mahomet Aquifer.

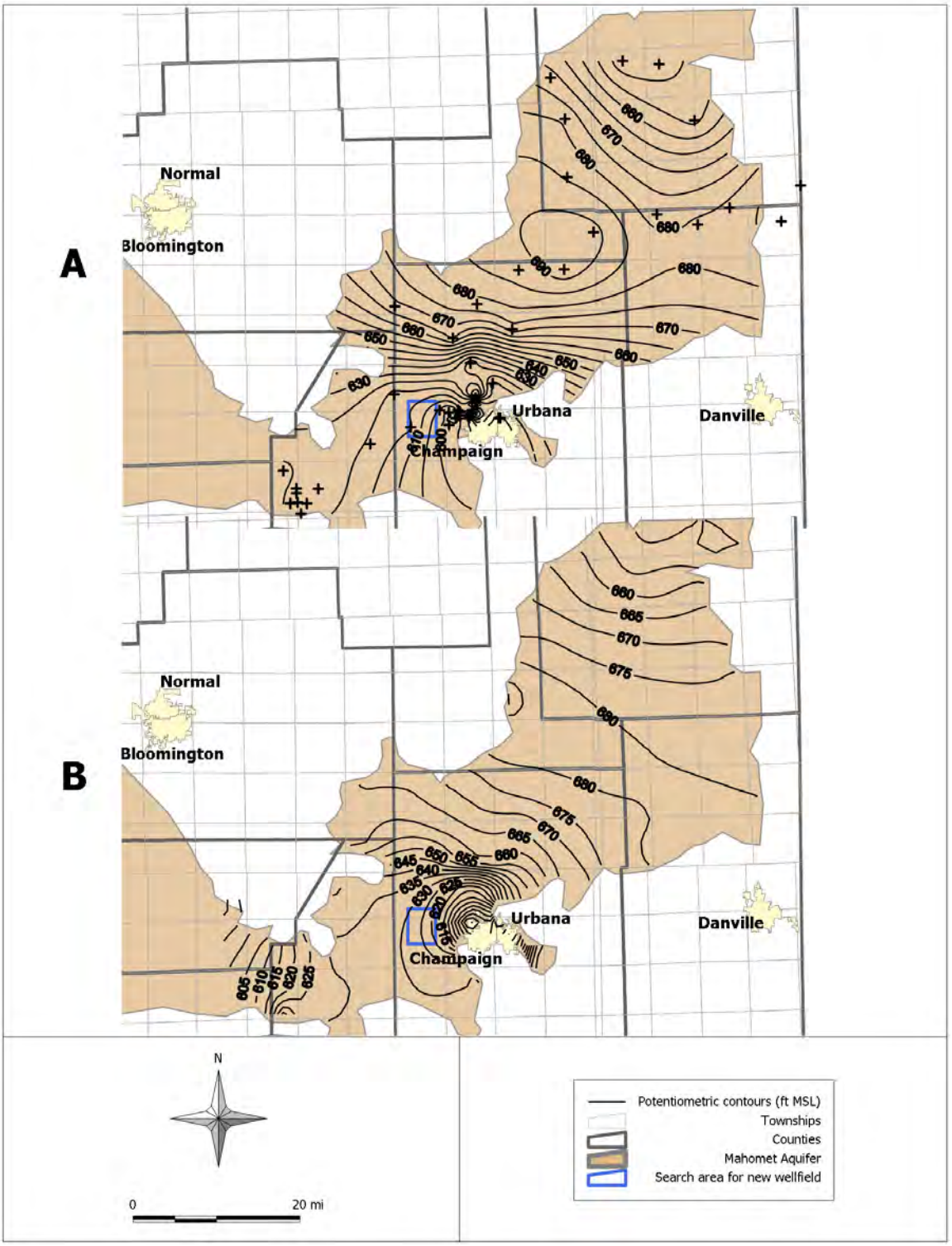

Figure 27: Comparison of measured (A) and modeled (B) water levels in the Mahomet Aquifer.

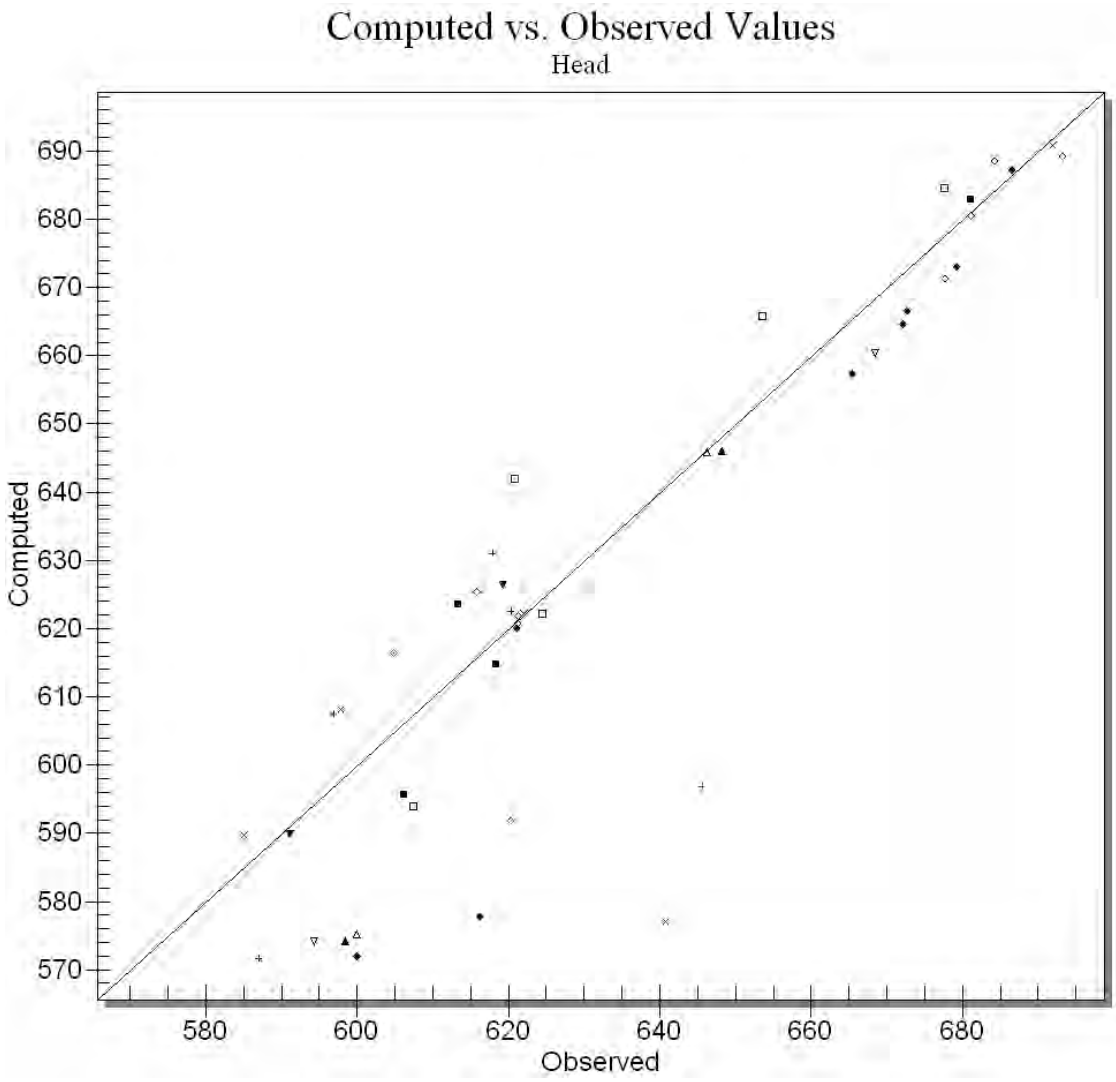

Figure 28: Measured versus modeled heads from the model calibration.

Table 20: Parameter values from the second conceptual model calibration

Parameter description	Calibrated value
Hydraulic conductivity	
Radnor Sand	10.0 ft/day
Vandalia Sand	41.5 ft/day
Non-aquifer in Layer 1	2.0 ft/day
Mahomet Aquifer	372 ft/day
Confining layer (Layer 2)	0.000227 ft/day
Low K zone in Mahomet Aquifer north of Champaign	11.0 ft/day
Recharge	
Recharge on Vandalia Sand	NA[1]
Recharge on non-aquifer material	NA
Recharge on Mahomet (Layer 3)	5.7E-5 ft/day
Recharge on Radnor Sand	NA
River cell conductance	
River conductance multiplier on Layer 1	2.83E-5 $ft/day \cdot ft$
Iroquois River (on Layer 3)	0.266 $ft^2/day \cdot ft$
Illinois River (on Layer 3)	596 $ft^2/day \cdot ft$
Other parameters	
Specific yield of Layer 1 (not varied)	0.1
Scale factor on Mahomet Aquifer pumpage	1.65

[1]Not applicable to this conceptual model - see Section 4.1.3

K - hydraulic conductivity. All layers were assumed to be isotropic ($K_x = K_y = K_z$).

Table 21: Summary of the net flow budget from the calibrated model.

	River cells	Recharge	Net to/from Layer 2	Wells
	Calibrated model of 2004 conditions			
Layer 1	0.53 in/yr	NA	-0.53 in/yr	0
Layer 3	-0.18 in/yr	0.25 in/yr	1.02 in/yr	53.7 MGD
	Calibrated parameters, net increase of 16 MGD in proposed wellfield			
Layer 1	0.66 in/yr	NA	-0.66 in/yr	0
Layer 3	-0.16 in/yr	0.25 in/yr	1.26 in/yr	69.7 MGD

Sign convention: + indicates net flow into the specified layer, - indicates net flow out of specified layer

5 New wellfield evaluation

We classified wells in the vicinity of the proposed wellfield based on the aquifer in which they are screened and defined an amount of drawdown due to pumping in the new wellfield that would likely necessitate lowering pumps in low–capacity wells. This was defined as two times the annual variation in water level measured in area wells, or approximately 12 ft. We also identified wells in which water levels may be drawn so low that they become dry due to limited depth. A series of wellfield configurations were compared in terms of these criteria.

5.1 Well interference assessment

The database of wells for Champaign and Piatt Counties was obtained from the ISGS. We reviewed logs of wells that are within 2–3 miles of the search area for the new wellfield (Figure 29). Of these wells, approximately 540 had enough information to determine which aquifer the well screen penetrates. Of the 540 wells, 220 are screened in the Glasford Aquifer and 320 are screened in the Mahomet Aquifer. The logs were classified according to the hydrogeologic units that could be identified.

Wells that are completed in the Glasford Formation are considered more vulnerable than those completed in the Mahomet Aquifer because water levels in the Glasford Formation could be lowered beneath the bottoms of wells completed in this formation. Figure 30 illustrates this point. The blue water levels represent conditions with none of the wells in the cross-section pumping. Recharge occurs both directly and diffusely to the Radnor Sand, so this unit has the highest water level. Pumping from the Mahomet Aquifer beyond the limits of the cross-section causes this unit to have the lowest water levels. The Vandalia Sand layer has an intermediate water level. The red water levels represent conditions when Well D is pumping from the Mahomet Aquifer. Drawdown is greatest in the pumped well and nearly as great in Well C, another Mahomet Aquifer well. Drawdown decreases vertically due the resistance to vertical flow from the Vandalia Sand to the Mahomet Aquifer and from the Radnor Sand to the Vandalia Sand. Although Well A has the smallest drawdown, it can be dried out because it is so shallow.

Water levels in the Mahomet Aquifer are anticipated to remain above the top of the aquifer, so water levels in wells completed in this formation will remain above the top of the screen. Pumps will likely have to be lowered in many of the Mahomet Aquifer wells to accommodate the lower water levels, but the wells are not anticipated to be rendered unusable.

For wells screened in layers above the Mahomet Aquifer, the available drawdown was estimated. Available drawdown was defined as the difference between the static water level in the well and a point 10 ft above the top of the well screen. Available drawdown was compared with the modeled drawdown in the layer representing the Mahomet Aquifer to determine if the well might be rendered unusable in a given scenario. It is an inherent assumption in our work that the drawdown in Glasford

Aquifer cannot exceed that in the Mahomet Aquifer. The forgoing analysis does not account for additional pumping from Decatur's Dewitt well field that may occur in drought conditions.

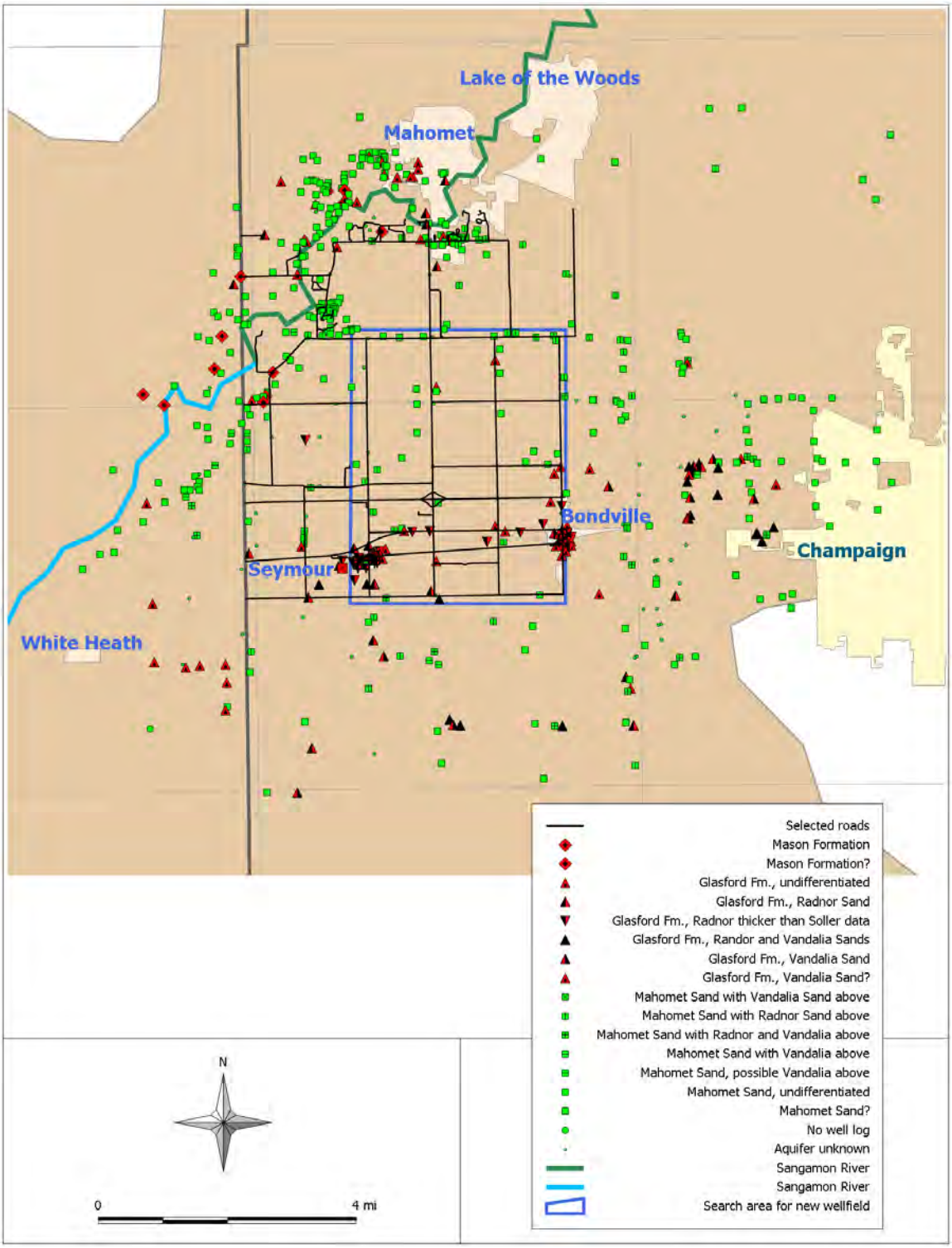

Figure 29: Location of wells from the ISGS database in the vicinity of the proposed wellfield.

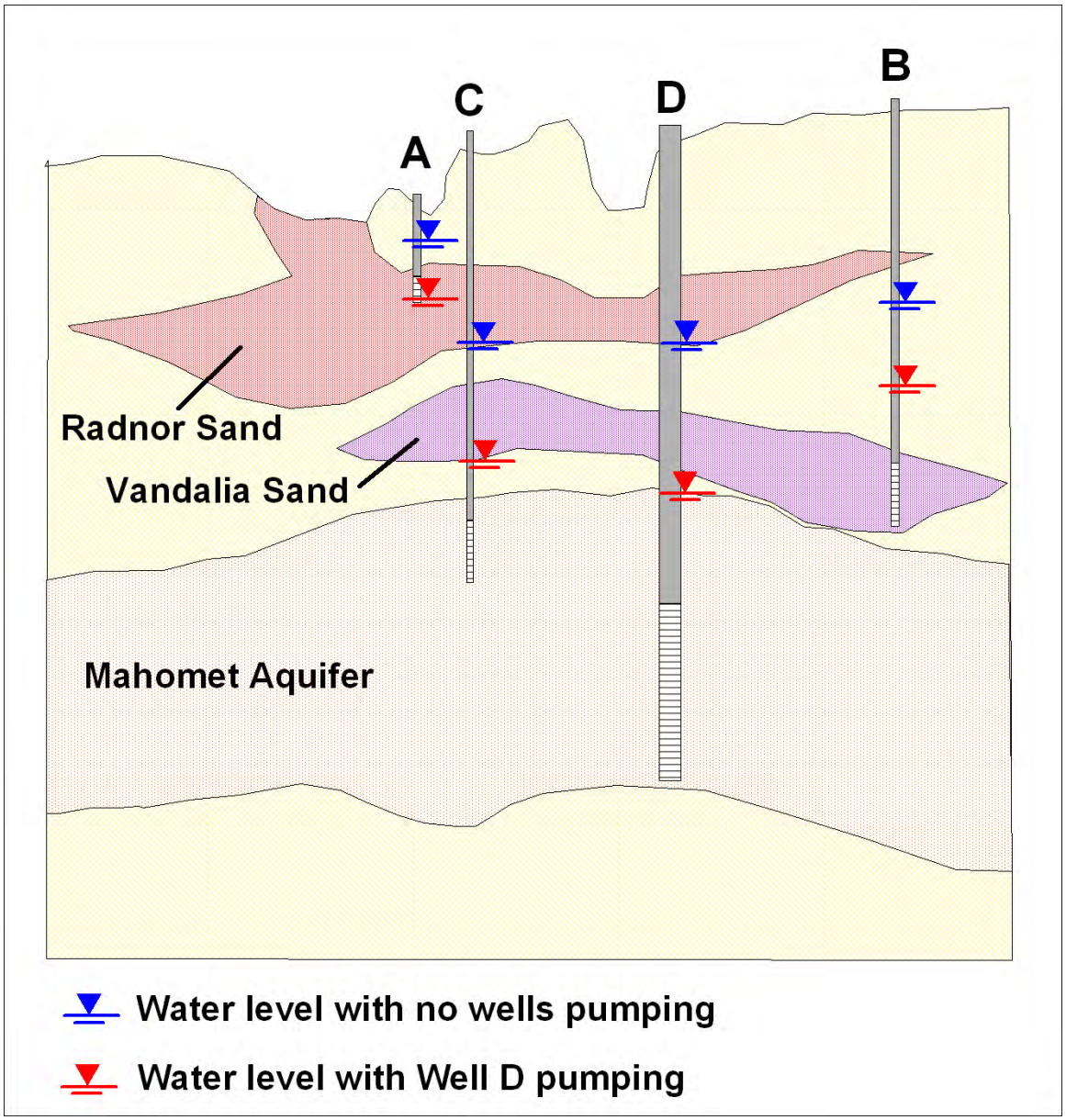

Figure 30: Well interference in various aquifers.

5.2 Wellfield design

The calibrated groundwater flow model described in Section 4 was used to compare candidate well locations within the search area (Figure 31). Based on reported capacities for Mahomet Aquifer wells in the area, a nominal capacity of 2.5 MGD (~1740 gpm) per well should be readily achievable. At that rate, the new wellfield would consist of a minimum of eight wells to produce 20 MGD. The new wellfield may include ILAW's Well 52, which has not yet been connected to the water supply.

5.2.1 Layout comparisons

Seven possible wellfield configurations were considered. Layouts were designed using the following rules:

- wells are to be located along existing roads,
- wells are to be located as far from existing wells as possible, and
- the center of the conceptual wellfield is to be located as close to the West Wellfield as is practical without causing excessive well interference, in order to minimize the cost associated with installing water mains.

Figure 32 shows a comparison of possible well locations within the search area. The drawdown due to a well pumping at each of the locations shown as black dots at a rate of 2.5 MGD was calculated. The information was summarized as the average drawdown in the Mahomet Aquifer beneath all known wells screened in the Glasford Formation (Figure 32A) and the the average drawdown in all known wells screened in the Mahomet Aquifer (Figure 32B).

Due to the concentration of Glasford wells near Bondville and Seymour (Figure 29), less interference with Glasford wells will result if a new well is located toward the northern limit of the search area. It should be noted that ILAW now provides water to these communities so many of these wells are likely no longer in use. Conversely, the southwestern corner of the search area is favored if interference with Mahomet wells is considered.

The configurations are described in the following list and shown schematically in Figure 33. Table 22 contains a comparison of the seven wellfield configurations in terms of the criteria described in Section 5.2.2.

1 nominal layout $\frac{3}{4} - mile$ spacing between wells, utilizing Well 52

2 denser layout $\frac{1}{2} - mile$ spacing, utilizing Well 52

3 #2 moved south $\frac{1}{2} - mile$ spacing, utilizing Well 52, along Bradley Avenue

4 #3 but denser $\frac{3}{8} - mile$ spacing utilizing Well 52, along Bradley Avenue

5 #4 without Well 52

6 very dense $\frac{3}{8} - mile$ spacing, shortest linear distance between wells

7 if pipe were free widest spacing in the search area

5.2.2 Evaluation criteria

Objective criteria identified that could be compared to differentiate the candidate wellfield layouts are listed below. Results of the comparisons are summarized in Table 22 and discussed in Section 5.2.4.

- the average drawdown in Mahomet Aquifer beneath Glasford Aquifer wells,
- average drawdown in Mahomet Aquifer wells,
- maximum drawdown in the Mahomet Aquifer beneath any Glasford Well,
- maximum drawdown in any Mahomet Aquifer Well, and
- the number of Glasford Aquifer wells in which the estimated drawdown will exceed the available drawdown estimated for the well.

5.2.3 Interference within the new wellfield

Pumping of each of the new wells will also reduce the available drawdown in the other new wells. This interference within the new wellfield was evaluated for Layouts 1, 6 and 7. For each simulation, the well with the most drawdown was turned off and the drawdown due to pumping of the other seven wells on this idle well was estimated. This is the total interference due to the other new wells pumping, which was 63.4 ft, 67.0 ft, and 59.5 ft, respectively. Moving from the minimum to maximum spacing is estimated to save 7.5 ft of available drawdown.

5.2.4 Discussion

Due to the high transmissivity of the Mahomet Aquifer, the modeled cone of depression associated with the proposed wellfield is broad and relatively shallow. In other words, drawdown due to pumping the well at steady–state rates is widespread (Figure 37). As a result, the average drawdowns beneath the wells considered in the well search are not strongly influenced by the layout of the wellfield. In fact, because the search area has relatively few Mahomet Aquifer wells near its center, the denser well configurations along Bradley Avenue (cases 3–5) have lower average drawdowns in Mahomet Wells than the other configurations. Conversely, impacts on Glasford Wells slightly favor cases 1,2, and 6. As noted above, ILAW now provides water to Seymour and Bondville so many of the wells in these communities are likely no longer in use.

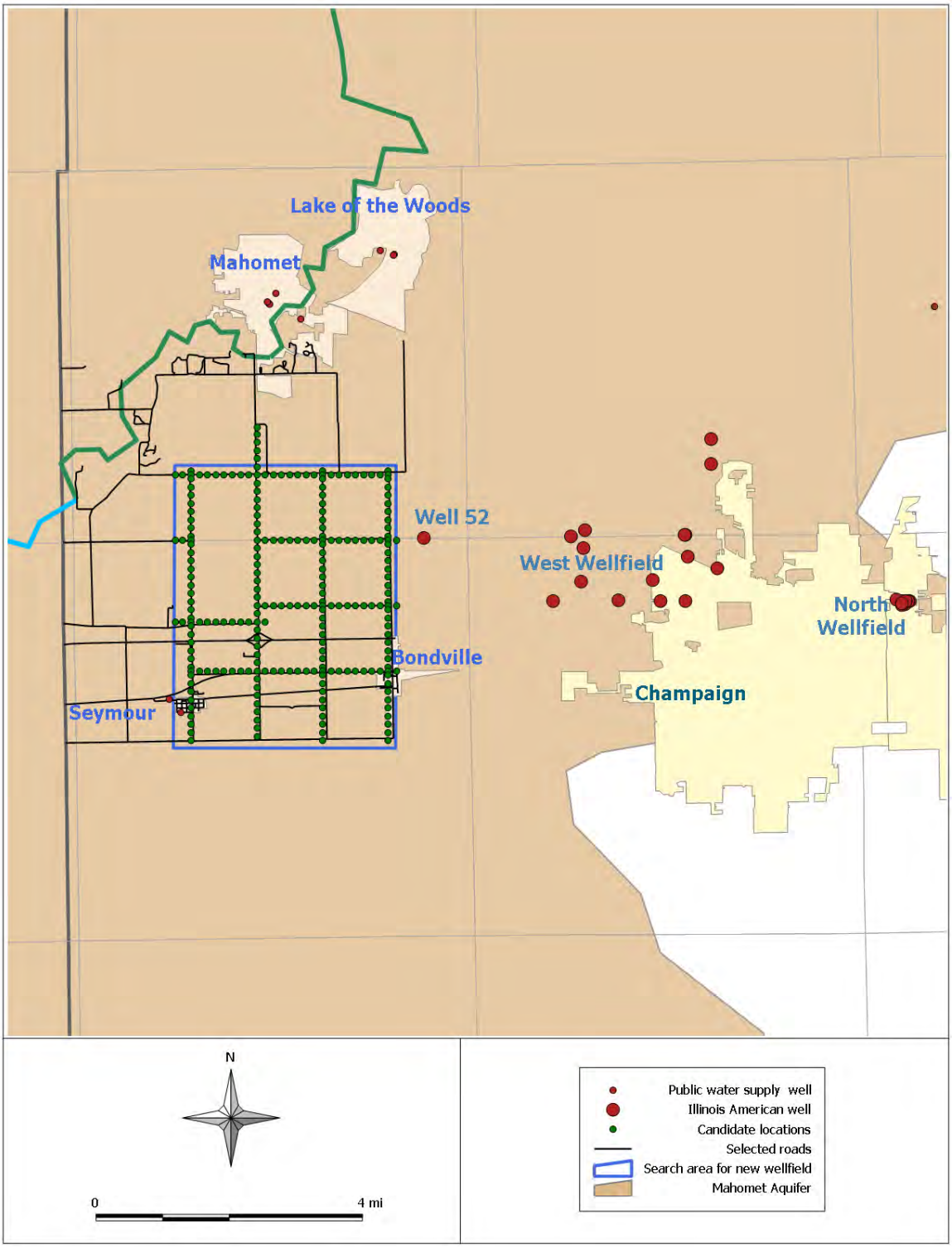

Figure 31: Locations considered for possible new wells in the search area.

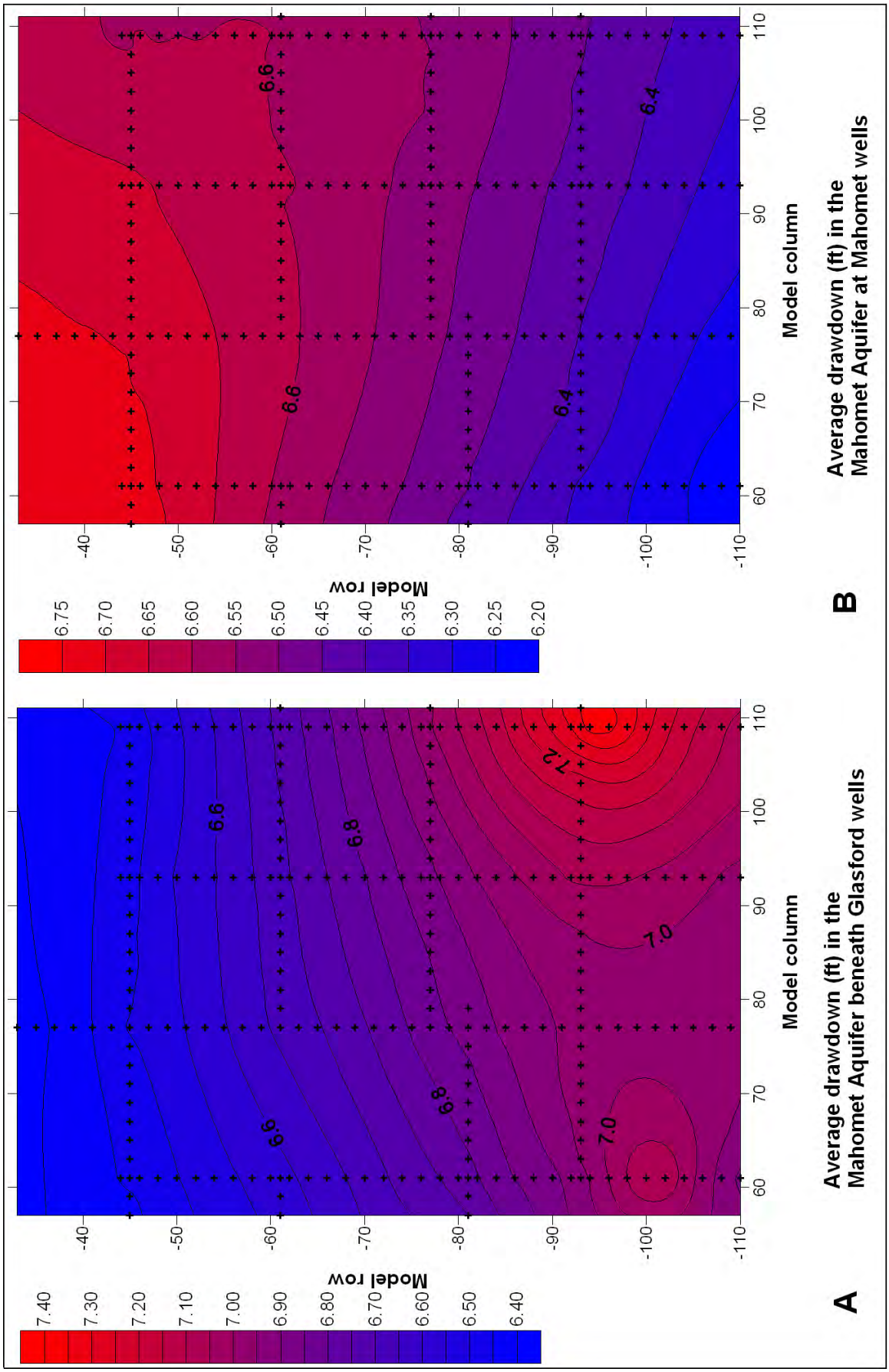

Figure 32: Evaluation of possible well locations in the search area.

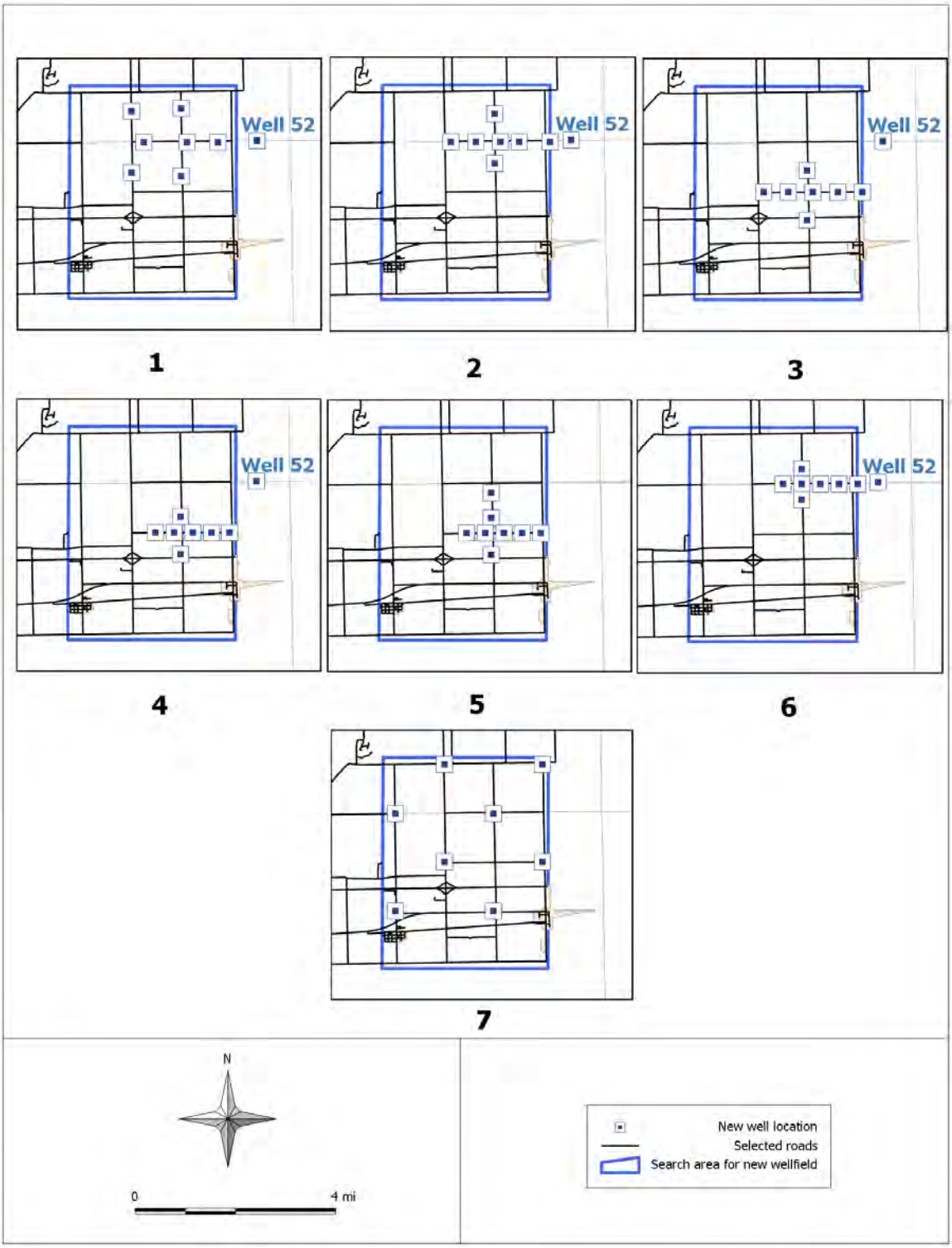

Figure 33: Wellfield configurations used for comparison.

Table 22: Comparison of the effects of wellfield layouts

case	$\bar{s}$ under Glasford wells	$\bar{s}$ in Mahomet wells	s_{max} under Glasford wells	s_{max} in Mahomet wells	Threatened Glasford wells
	Calibrated parameters, net 16 *MGD*				
1	50	49.3	61.5	61.5	65
2	50.1	49.3	61.1	63.7	65
3	51.7	48.9	63.5	64.6	66
4	51.8	48.9	65	66.1	67
5	51.9	48.9	64.9	66.6	69
6	50.1	49.2	62.7	65.1	65
7	50.8	49	59.9	57.2	66
	Worst-case parameters, net 16 *MGD*				
1	73.8	73	85.4	85.5	136
2	73.9	73	85	87.7	135
3	75.5	72.6	87.6	88.7	136
4	75.6	72.6	89.1	90.2	136
5	75.7	72.6	89	90.7	136
6	73.9	73	86.7	89.1	135
7	74.6	72.6	83.8	81.2	135

$\bar{s}$ - average drawdown

s_{max} - maximum drawdown

6 Estimates of wellfield impact

We estimated historical pumping rates from the Mahomet Aquifer and used the groundwater flow model to estimate water levels in the aquifer over time. Based on the results of the wellfield comparisons described in Section 5.2, Layout 1 was then used in a series of simulations of development of the new wellfield over the next 30+ years. These scenarios are simulated at steady-state. We then evaluated the influence of the seasonal nature of the the withdrawal to see if the steady-state models may over-predict the amount of drawdown caused by a given scenario. Using this layout and the proposed pumping rates, the a new well field West of Champaign would provide the needed water and would be sustainable for the next 25 years of pumping. This conclusion is based on assumptions we made about growth in groundwater use in the area. These growth scenarios do not include additional high capacity wells pumping from the Mahomet Aquifer near the proposed well field.

6.1 Water levels over time

In order to put additional groundwater development at the Champaign Operation into perspective, we estimated historical annual average pumping rates from the Mahomet Aquifer and used the model to estimate water levels in the aquifer over time. Table 23 summarizes the simulated discharge rates for Mahomet Aquifer wells. Assumptions and sources for the data in Table 23 are listed below.

- Prior to development in the area (some time before 1890 based on Figure 16 of Visocky and Schicht [1969]), no withdrawal occurred from the Mahomet Aquifer.
- As of 1945, estimated withdrawal from the Mahomet Aquifer was about 4 *MGD* based on Figure 16 of Visocky and Schicht [1969]. None of this withdrawal was in the Champaign/Urbana area based on Figure 20 of Visocky and Schicht [1969].
- As of 1965, estimated withdrawal from the Mahomet Aquifer was about 20 *MGD* based on Figure 16 of Visocky and Schicht [1969]. Approximately 13 *MGD* of this withdrawal was in the Champaign/Urbana area based on Figure 20 of Visocky and Schicht [1969].
- The total withdrawal from the Mahomet Aquifer in 1985 was estimated as the average of the value discussed above for 1965 and the calibrated model value of 53.7 *MGD*. The value reported for ILAW's withdrawal in the Champaign Operation for 1992 was used as representative of 1985.
- Withdrawal for 2004 was taken from the calibrated model described in Section 4.2.5.
- Withdrawal representing conditions in the year 2025 is described in Section 6.2.

Modeled water levels in the Mahomet Aquifer through the search area for the new wellfield and West Wellfield are shown in Figure 34. Pre-development water levels in this area were modeled

to be slightly above land surface on the western end of the cross-section to 40 to 70 ft below ground surface on the eastern end. Water level declines in this cross-section are caused by the overall increase in withdrawal from the aquifer and, to a greater extent, by development of ILAW's Mahomet Aquifer wells. For comparison, the last line in Table 23 is the modeled decline in water level (drawdown) at the eastern end of the cross-section. For the calibrated parameter set, the decline from 2004 to 2025 was estimated to be less than that from 1985 to 2004 and about the same magnitude as the decline from pre-development to 1965.

Water levels were predicted to remain above the top of the Mahomet Aquifer except in the simulation using the worst-case parameter set. In other words, the Mahomet Aquifer remains saturated in all of the scenarios except the worst case.

Table 23: Average annual pumping rates (in *MGD*) used in the historical simulations

Year	Predevelopment	1945	1965	1985	2004	2040
Well group						
North Wellfield	0.0	0.0	2.2	2.2	2.2	2.2
West Wellfield	0.0	0.0	10.8	15.8	32.9	28.9
New Wellfield	0.0	0.0	0.0	0.0	0.0	20.0
Other wells[1]	0.0	4.0	7.0	12.8	18.6	18.6
Total	0.0	4.0	20.0	30.8	53.7	69.7
Incremental increase		4.0	16.0	10.8	22.9	16.0
ILAW increase		0.0	13.0	5.0	17.1	16.0
Total drawdown (ft)[2]		1.4	41	59	120	160/180

[1]Other wells are all other wells in the model besides ILAW wells.

[2]Drawdown calculated at the eastern end of the cross-section shown in Figure 34

6.2 Development scenarios

Development of the new wellfield is anticipated to take place gradually. ILAW estimates the rate of growth in demand to be 1.7 percent per year. Four simulations were run with the calibrated parameter set to estimate the changes in water level (drawdown) in response to this development. Table 24 summarizes the distribution of pumping among groups of wells in the model. Predicted effects of this development are illustrated as drawdown relative to modeled conditions for 2004. The following list describes the scenarios.

1. Redistribution of current rates of pumping in the Champaign Operation. Five *MGD* is shifted from the West Wellfield to the new wellfield. This scenario represents conditions from 2006

to about 2011 (see Figure 35). During this period, at the expected rate of growth, ILAW's demand will increase by less than 2 *MGD*. Note that the modeled drawdowns around the West Wellfield are negative because no net increase was modeled but some withdrawal was shifted away from the West Wellfield.

2. An increase of 5 *MGD* in total withdrawal occurs from the year 2006 to 2019. This increased withdrawal is added to the new wellfield (see Figure 36A).

3. An additional increase of 5 *MGD* in total withdrawal occurs from the year 2019 to 2029. This increased withdrawal is added to the new wellfield (see Figure 36B).

4. An additional increase of 6 *MGD* in total withdrawal occurs from the year 2029 to 2040. This increased withdrawal was divided between the West Wellfield (1 *MGD* increase) and the new wellfield (5 *MGD*). Drawdowns were estimated using the calibrated model parameters (Figure 37A) and the worst-case model parameters (Figure 37B).

Table 24: Pumping rates (in *MGD*) used in the forward simulations

Scenario	Calibrated model	Scenario 1	Scenario 2	Scenario 3	Scenario 4
Ending year	2004	2011	2019	2029	2040
Well group					
North Wellfield	2.2	2.2	2.2	2.2	2.2
West Wellfield	32.9	27.9	27.9	27.9	28.9
New Wellfield	0.0	5.0	10.0	15.0	20.0
Other wells	18.6	18.6	18.6	18.6	18.6
Total	53.7	53.7	58.7	63.7	69.7

6.3 Steady-state versus transient effects

A comparison was made between modeled steady–state drawdowns and transient drawdowns based on the seasonal variation in withdrawal described in Section 2.3.3. The growing season was assigned to the period May through August. It was assumed that over the eight months between growing seasons, water levels would reach a steady–state. As described in Section 4.2.5 and shown in Table 24, the maximum total pumping in the steady–state model of the proposed wellfield is 69.7 *MGD*. This represents an annual average rate. Assuming a ratio for growing season to off–season pumping of 2:1 results in seasonal average rates of 104.2 *MGD* and 52.1 *MGD*, respectively. Table 25 lists the assumed distribution of this seasonal pumping among groups of wells in the model. The discharge

values used for the ILAW wellfields in the steady–state model were higher than the annual average rates described in Section 2.1 because the pumping in these and other wells was scaled up to account for pumpage from unknown wells (see Section 4.2.1).

A steady–state model of the pumping rates representing off–season conditions set the starting heads for a transient simulation of the growing season. Water levels drop throughout the transient simulation, but in general do not drop to the levels indicated by the steady–state simulation. This is illustrated in Figure 38, which is a contour map of the difference between modeled heads at the end of the transient simulation and those from the steady–state simulation. Positive values indicate higher heads (less drawdown) at the end of the transient model. In the near–field, the heads at the end of the transient simulation were approximately 2 ft to 6 ft higher than the steady–state simulation. This difference is sensitive to the value used for the specific yield of Layer 1. In order to be conservative, the specific yield value was decreased from that used in the model calibration (0.10) to a value much lower than would be expected for an unconfined aquifer (5×10^{-4}). In the far–field, scaled–up pumping of wells resulted in more drawdown locally in the transient model than the steady–state model. These results suggest that the steady–state model is a reasonable approximation of conditions near the Champaign Operation, but tends to over–predict drawdowns in the far field.

Table 25: Well discharges used in the comparison of steady-state and transient drawdowns

Well group	Combined discharge MGD		
	Steady-state model	Off-season	Growing Season
ILAW West wellfield	28.9	14.7	29.4
ILAW North wellfield	2.2	1.6	1.6
Proposed ILAW wellfield	20.0	10.0	20.0
Irrigation wells	0	0	11.2
Other wells	18.6	25.8	42.0
Total	69.7	52.1	104.2

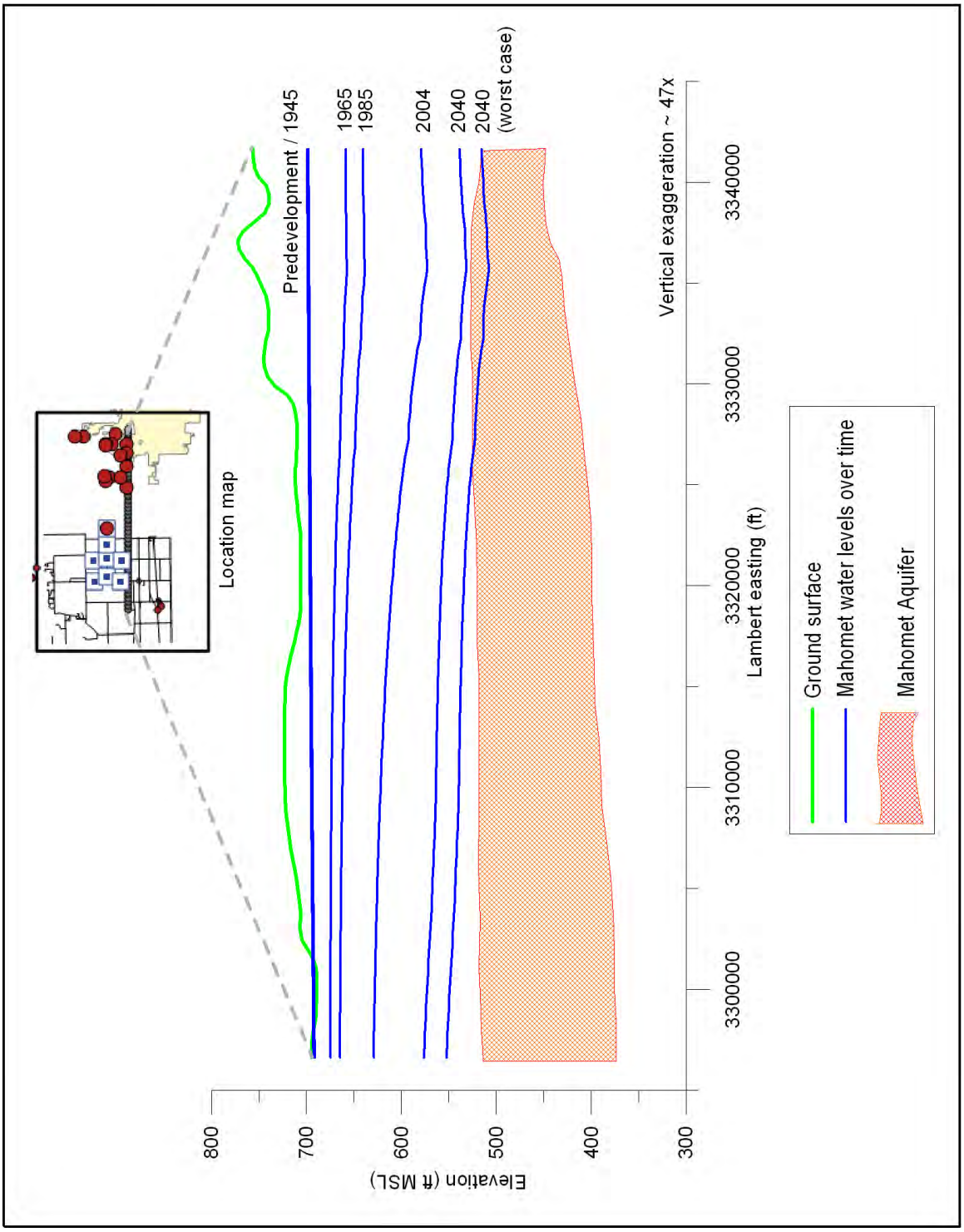

Figure 34: Cross-section of simulated historical water levels and projected levels for the year 2025.

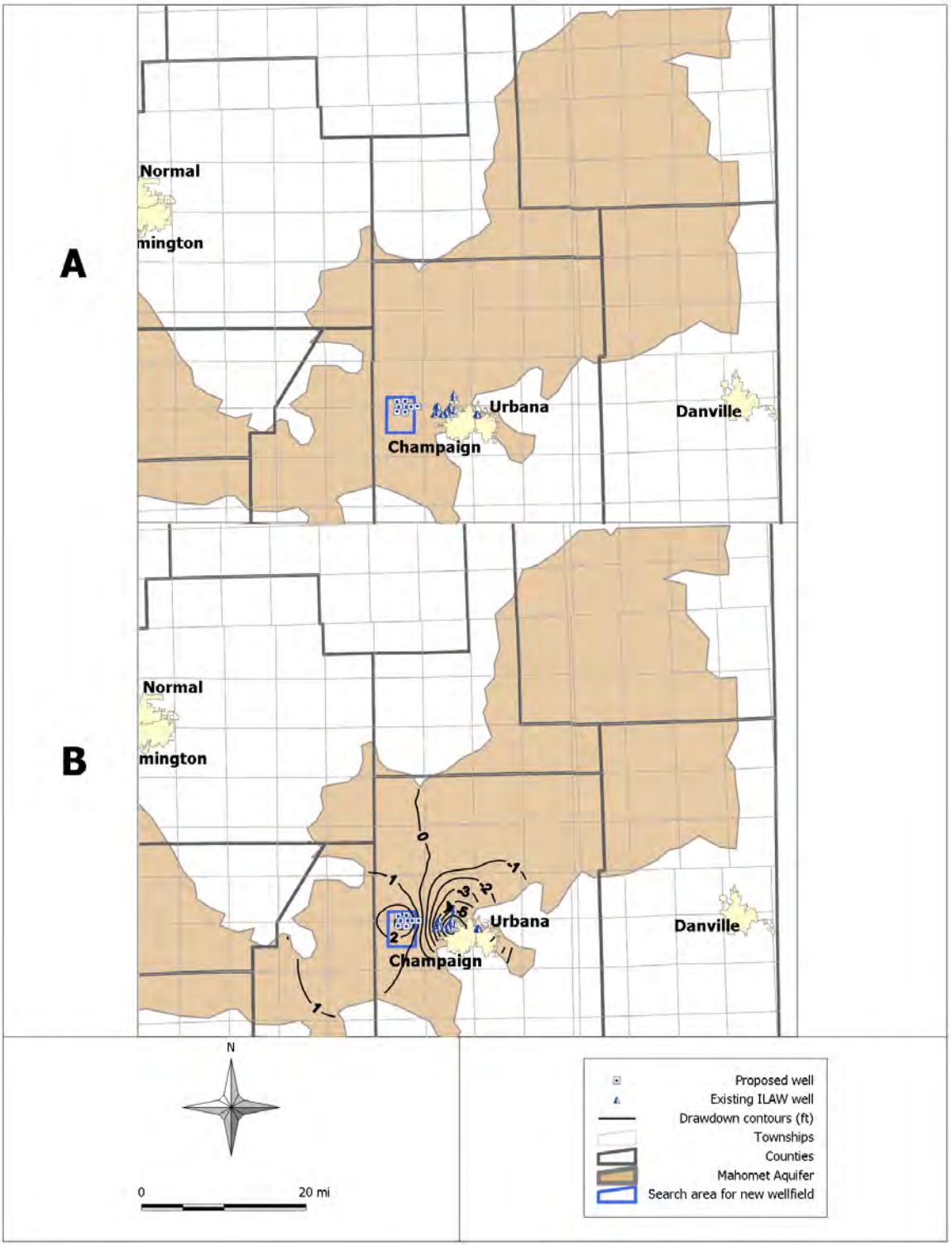

Figure 35: Base map (A) and modeled drawdowns for the year 2011 (B).

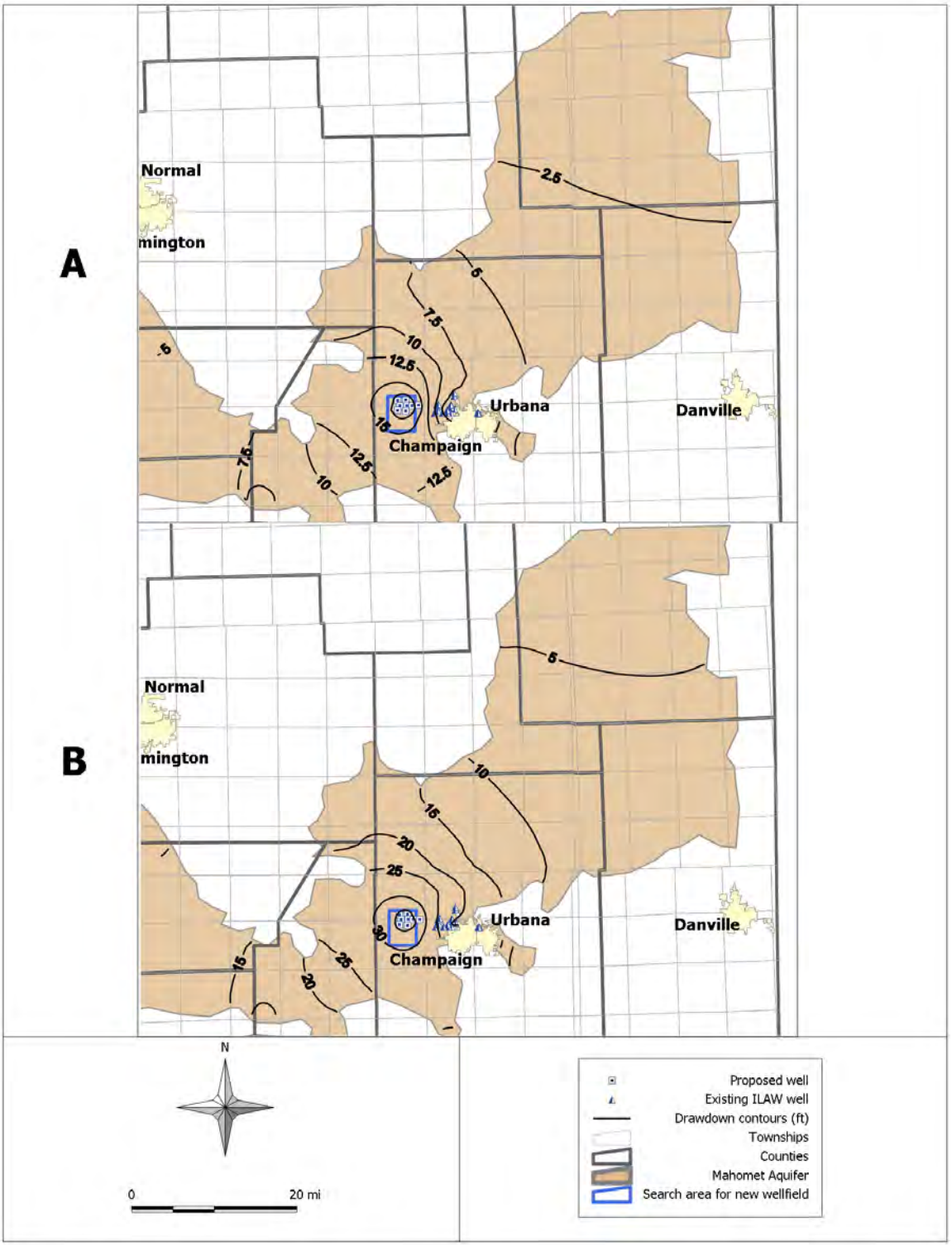

Figure 36: Modeled drawdowns with the calibrated parameters for the years 2019 (A) and 2029 (B).

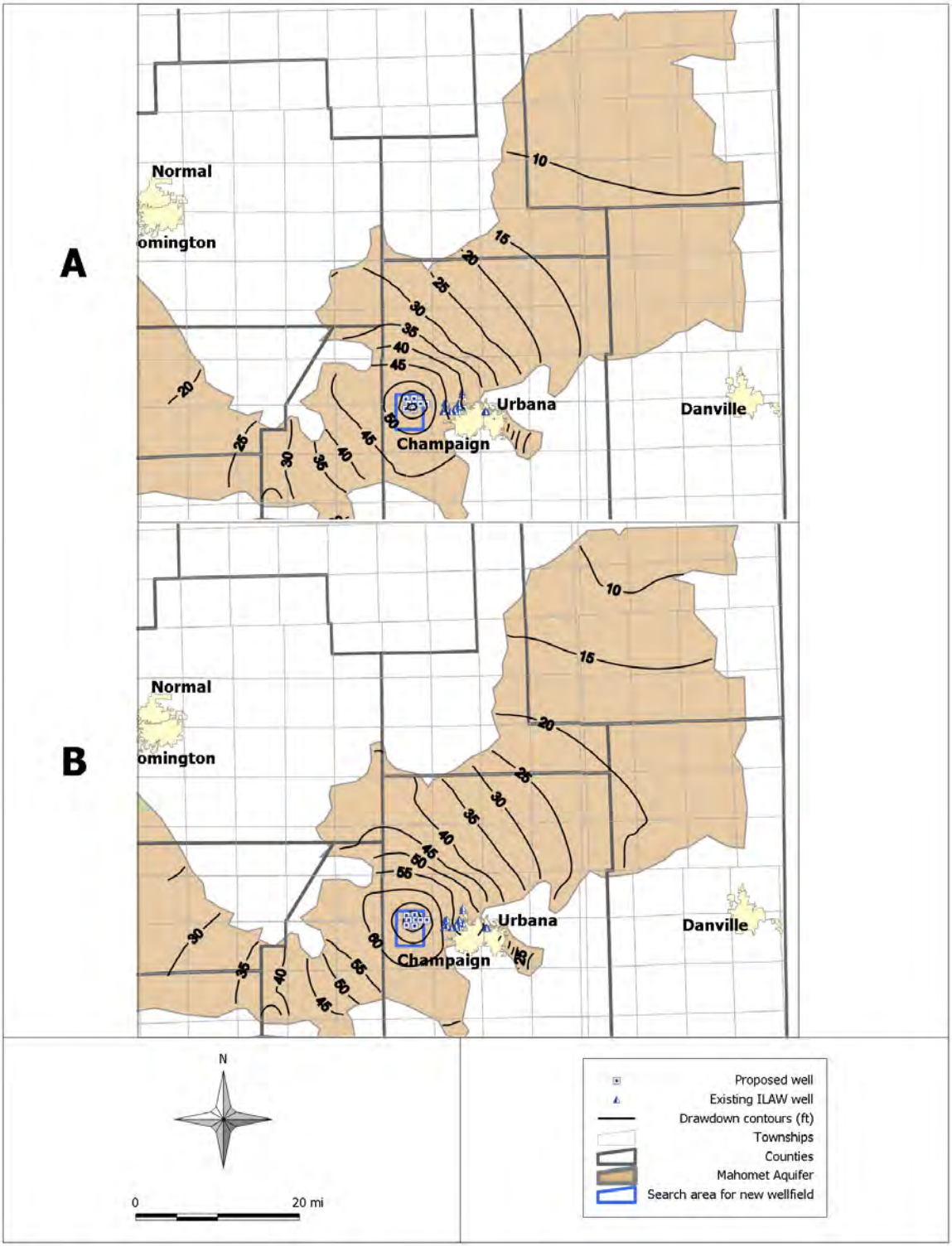

Figure 37: Modeled drawdowns with the calibrated (A) and worst-case parameters (B) for the year 2040.

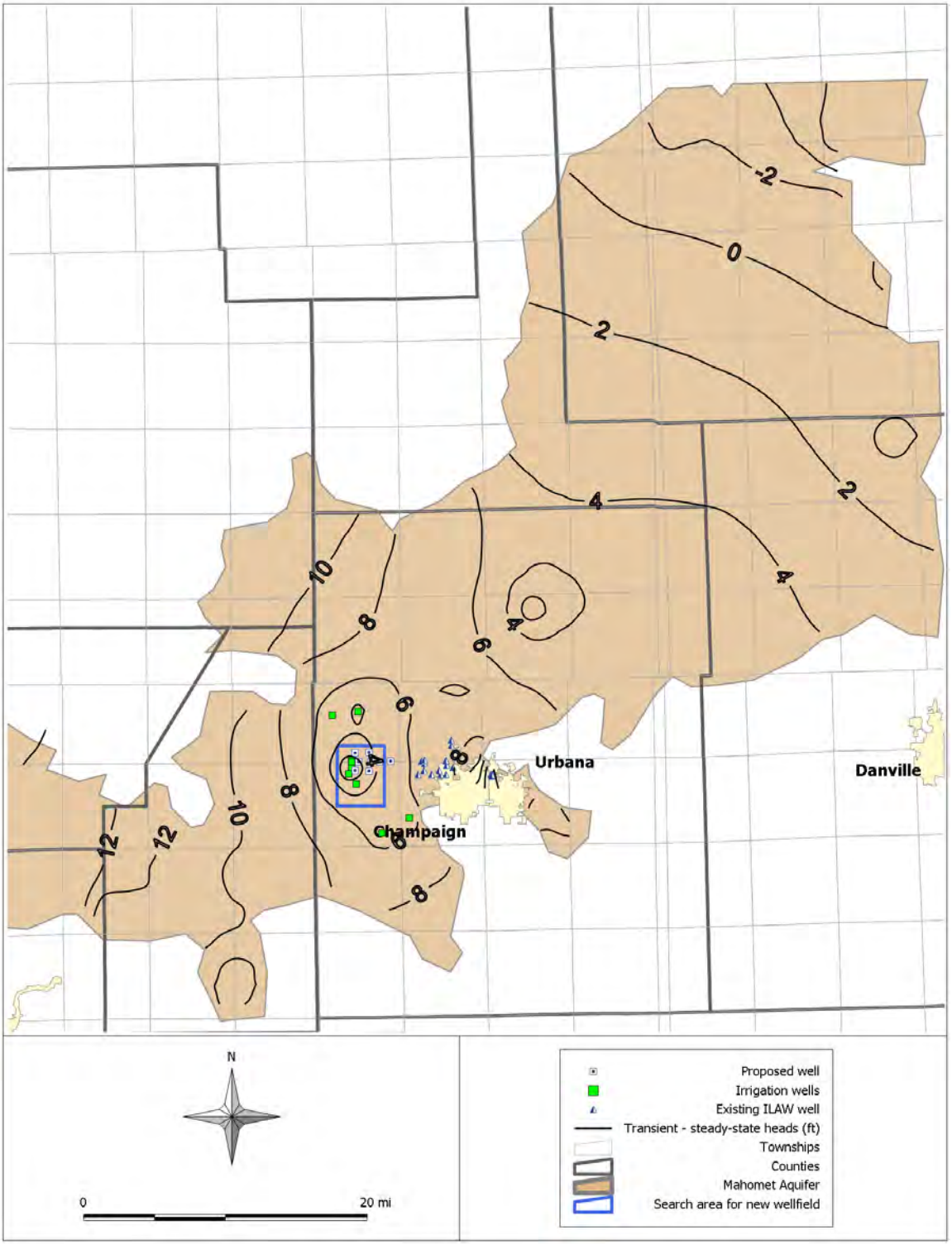

Figure 38: Comparison between steady-state heads and heads from the end of a transient model of the growing season.

7 Conclusion and recommendations

The modeling analysis, supported by the local data, suggests that the new wellfield can be a sustainable supply at its planned future pumping rate. The regional water demand analysis described in this report shows that other users' withdrawal from the Mahomet Aquifer will increase over time, perhaps dramatically if municipalities not located above the aquifer shift their sources of supply to the aquifer. This increase in withdrawal will reduce the capacity of the aquifer system to yield water in the Champaign/Urbana area and will exacerbate the effects of expansion of the ILAW source of supply. In other words, the sustainability of Champaign/Urbana public water supply will be determined by the combined water use in the region. Conservation measures should be implemented by all users of the resource.

Dewatering of water–bearing zones above the Mahomet Aquifer will affect local wells and will likely reduce the capacity of the Mahomet Aquifer due to decreased vertical leakage. A system of monitoring wells in the Glasford Aquifer will allow ILAW to understand this trend. Results of the ISWS's Glasford Well survey should be incorporated as they become available. Water level data from this survey will be useful in further calibrating the model.

Groundwater flow modeling described in this report suggests that the impact of development of a new wellfield west of Champaign will be widespread and not extremely sensitive to the layout of the wellfield. It has been observed elsewhere in the Mahomet Aquifer that the 3–dimensional complexity of the aquifer dictates how water flows through the system. A prototype wellfield should be constructed and monitored to determine the actual impact and ultimate design of the wellfield. The groundwater flow model developed for this report should then be updated with information from the prototype wellfield and used to determine whether additional wells are required and if so, determine if they can be placed between existing wells or must be located further out to avoid excessive interference.

The recommended wellfield design is shown in Figure 39. This design utilizes Well 52 and calls for initial installation of five new wells. We recognize that logistical considerations may alter this layout. A long–term test should be performed using these wells (or long–term monitoring of their actual operation). Data from the actual operation of these initial wells and actual decline in water levels in the Mahomet and Glasford aquifers should be utilized to determine whether the wellfield can be completed by filling in between the initial wells or if the wellfield must be expanded to limit its impact on existing wells.

Monitoring data from operation of the wellfield should also be used to determine the effective specific yield of the Glasford Formation so transient simulations can be made with more certainty. Transient models could be used to develop wellfield operation plans with respect to maximizing infiltration from the Sangamon River during periods of excess river discharge or other criteria.

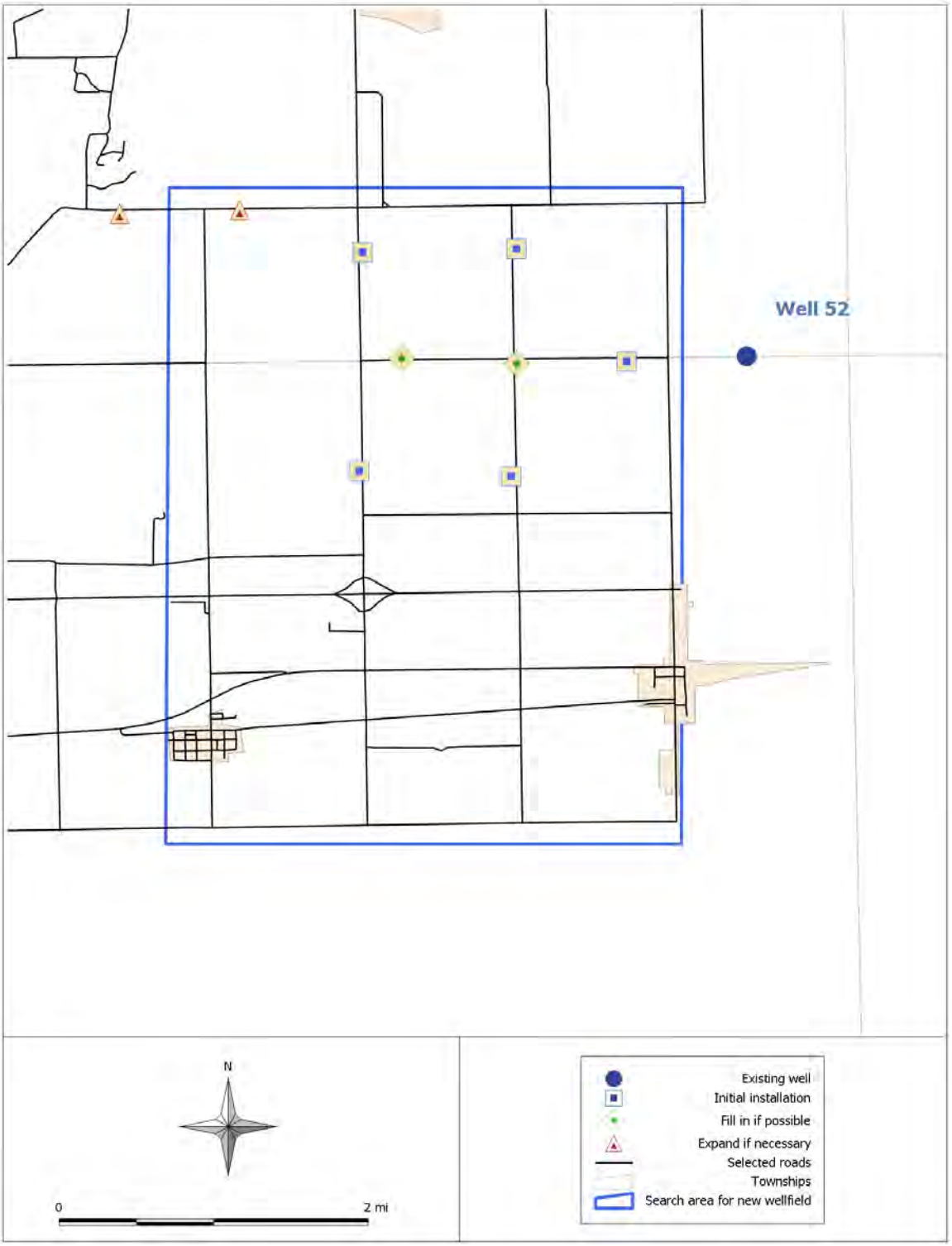

Figure 39: Recommended layout for the new wellfield.

References

[Doherty, 2004] Doherty, J. (2004). PEST - model-independent parameter estimation user manual. Software manual.

[Dzielgielewski et al., 2005] Dzielgielewski, B., Yang, X., Bik, T., Margono, H., and Richey, M. (2005). County Level Forecasts of Water Use in Illinois: 2005-2025. Technical report, Southern Illinois University - Carbondale and Illinois State Water Survey.

[Haitjema et al., 2001] Haitjema, H. M., Kelson, V., and de Lange, W. (2001). Selecting MODFLOW cell sizes for accurate flow fields. *Ground Water*, 39(6):931–938.

[Hantush and Jacob, 1955] Hantush, M. and Jacob, C. (1955). Non-steady radial flow in an infinite leaky aquifer. *Transactions of the American Geophysical Union*, 36:95–100.

[Harbaugh et al., 2000] Harbaugh, A., Banta, E., Hill, M., and McDonald, M. (2000). MODFLOW-2000, The U.S. Geological Survey Modular Ground-water Model - User Guide to Modularization Concepts and the Ground-water Flow Process. Open-File Report 00-92, U.S. Geological Survey.

[ISU, date] ISU (no date). Population projections for the state and counties of Illinois, 1990-2020. Technical report, Illinois State University Census and Data User Services.

[ISWS,] ISWS. Center for groundwater science - mahomet aquifer general information. accessed January 25, 2006.

[ISWS, 2005] ISWS (2005). Illinois water inventory program - annual public water supply pumping data: 1979-2004.

[Kempton et al., 1991] Kempton, J., Johnson, W., Hwigold, P., and Cartwright, K. (1991). *Mahomet Bedrock valley in east-central Illinois; topography, glacial drift stratigraphy, and hydrogeology.* Special Paper 258.

[Kruseman and de Ridder, 1991] Kruseman, G. and de Ridder, N. (1991). *Analysis and Evaluation of Pumping Test Data*. International Institute for Land Reclamation and Improvement, Waneningen, The Netherlands, second edition.

[Larson et al., 2003a] Larson, D., Herzog, B., and Larson, T. (2003a). Groundwater geology of DeWitt, Piatt, and Northern Macon Counties, Illinois. Technical report, Illinois State Geological Survey.

[Larson et al., 2003b] Larson, D., Mehnert, E., and Herzog, B. (2003b). The Mahomet Aquifer - A Transboundary Resource in East-central Illinois. *Water International*, 28(2):170–180.

[McDonald and Harbaugh, 1988] McDonald, M. and Harbaugh, A. (1988). *A modular three–dimensional finite–difference ground–water flow model*. Number 6, Chapter A1.

[NOAA, 2003] NOAA (2003). US daily station normals: 1971-2000 (clim84). Technical report, National Oceanic and Atmospheric Administration.

[Panno et al., 1994] Panno, S., Hackley, K., Cartwright, K., and Lui, C. (1994). Hydrochemistry of the Mahomet Bedrock Valley Aquifer, east-central Illinois: indicators of recharge and ground-water flow. *Ground Water*, 32(4):591–604.

[Roadcap and Wilson, 2004] Roadcap, G. and Wilson, S. (2004). Analysis of an aquifer test at Decatur #2 and implications for the interaction between the Mahomet Aquifer and the Sangamon River. Technical report, Internal Report, Illinois State Water Survey.

[Soller et al., 1999] Soller, S., Kempton, J., and Berg, R. (1999). Three-dimensional geologic maps of quaternary sediments in east-central Illinois. Technical report, U.S. Geological Survey, Illinois State Geological Survey. Geologic Investigation Series Map I-2669.

[Visocky and Schicht, 1969] Visocky, A. and Schicht, R. (1969). Groundwater resource of the Buried Mahomet Aquifer Bedrock Valley. Report of Investigation 62.

A Additional water demand results tables

Additional data tables are provided from the water demand section. The tables show the raw data used in the graphs and/or calculations of the water demand projections presented in Section 2.

Table 26: Population projections per county [ISU, date, Dzielgielewski et al., 2005].

County	**2000**	**2005**	**2010**	**2015**	**2020**	**2025**
Cass	13695	13374	12967	12793	12718	12644
Champaign	179669	186234	195752	201810	207331	213002
DeWitt	16798	16546	16253	16033	15874	15717
Ford	14241	14177	14075	13940	13804	13671
Iroquois	31334	30757	30075	29795	29611	29428
Logan	31183	31763	32166	32473	32669	32866
Macon	114706	114516	114242	114597	114845	115093
Mason	16038	15443	14911	14568	14469	14370
McLean	150433	156861	162357	167370	171641	176021
Menard	12486	13772	14879	16082	17522	19091
Piatt	16365	16555	16699	16946	17347	17757
Tazewell	128485	129922	130233	130857	132465	134093
Vermilion	83919	84324	84471	84872	85640	86414
Woodford	35469	36869	38226	40238	42756	45431

Table 27: Percent population growth projections in each county. Calculated from [ISU, date, Dzielgielewski et al., 2005]

County	Percent change				
	2005	**2010**	**2015**	**2020**	**2025**
Cass	-2.34	-3.05	-1.34	-0.59	-0.58
Champaign	3.66	5.11	3.09	2.74	2.73
DeWitt	-1.49	-1.78	-1.34	-1.00	-0.99
Ford	-0.44	-0.71	-0.95	-1.02	-0.95
Iroquois	-1.84	-2.21	-0.94	-0.62	-0.61
Logan	1.86	1.27	0.96	0.61	0.60
Macon	-0.16	-0.24	0.30	0.22	0.22
Mason	-3.71	-3.44	-2.30	-0.67	-0.69
McLean	4.28	3.50	3.09	2.55	2.56
Menard	10.30	8.04	8.09	8.95	8.97
Piatt	1.16	0.87	1.48	2.36	2.37
Tazewell	1.12	0.23	0.48	1.23	1.23
Vermilion	0.48	0.18	0.47	0.91	0.90
Woodford	3.95	3.68	5.26	6.26	6.26

B Model input files

A compact disc containing the model input files for the MODFLOW model runs described in this report was provided to the Illinois State Water Survey. See the file read_me_ISWS.txt for a description of the disc contents and other information about the model files.

Table 28: Self-supplied domestic population per county.

County	2000	2005	2010	2015	2020	2025
Cass	5605	5474	5307	5236	5205	5175
Champaign	13649	14148	14871	15331	15751	16181
DeWitt	5768	5682	5581	5506	5451	5397
Ford	3821	3804	3777	3741	3703	3668
Iroquois	7504	7366	7203	7135	7091	7048
Logan	9913	10097	10225	10323	10386	10448
Macon	5096	5088	5076	5091	5102	5113
Mason	7998	7701	7436	7265	7216	7166
McLean	20813	21703	22463	23156	23747	24354
Menard	3496	3856	4166	4503	4906	5346
Piatt	5685	5751	5801	5887	6026	6169
Tazewell	16945	17135	17175	17258	17470	17685
Vermilion	19299	19392	19426	19518	19695	19873
Woodford	22099	22971	23817	25070	26639	28306

Table 29: Acres of cropland projections per county.

County	2000	2005	2010	2015	2020	2025
Cass	152744	141011	130180	120180	110949	102426
Champaign	543427	534414	525550	516834	508231	499831
DeWitt	194712	190770	186907	183122	179414	175781
Ford	306557	317264	328345	339812	351681	363964
Iroquois	632924	630909	628899	626896	624900	622909
Logan	363588	368778	374042	379382	384797	390290
Macon	301783	299907	298043	296190	294349	292520
Mason	264143	263688	263233	262779	262326	261874
McLean	655885	639537	623596	608052	592896	578118
Menard	151766	149955	148164	146396	144648	142921
Piatt	243438	240521	237639	234792	231979	229200
Tazewell	300357	292159	284185	276428	268883	261544
Vermilion	456220	453399	450594	447807	445037	442285
Woodford	276597	278846	281114	283400	285705	288028

Table 30: Acres of irrigated cropland projections per county [Dzielgielewski et al., 2005].

County	2005	2010	2015	2020	2025
Cass	9914	10416	10783	11032	11179
Champaign	4889	4810	4733	4657	4582
DeWitt	856	848	840	832	824
Ford	668	690	713	736	761
Iroquois	6536	8119	9692	11255	12808
Logan	549	557	564	572	579
Macon	467	471	476	480	485
Mason	96890	104457	111996	119510	126997
McLean	936	918	901	884	868
Menard	966	955	944	934	924
Piatt	334	362	390	416	442
Tazewell	42256	48963	55273	61203	66767
Vermilion	144	144	144	144	143
Woodford	504	478	451	424	397

Table 31: Acres of irrigated cropland projections overlying the Mahomet Aquifer.

County	2005	2010	2015	2020	2025
Cass	4461	4687	4852	4964	5031
Champaign	3227	3175	3124	3074	3024
DeWitt	556	551	546	541	536
Ford	240	248	257	265	274
Iroquois	4444	5521	6591	7653	8709
Logan	329	334	338	343	347
Macon	168	170	171	173	175
Mason	96890	104457	111996	119510	126997
McLean	337	330	324	318	312
Menard	270	267	264	262	259
Piatt	234	253	273	291	309
Tazewell	36340	42108	47535	52635	57420
Vermilion	50	50	50	50	50
Woodford	131	124	117	110	103